

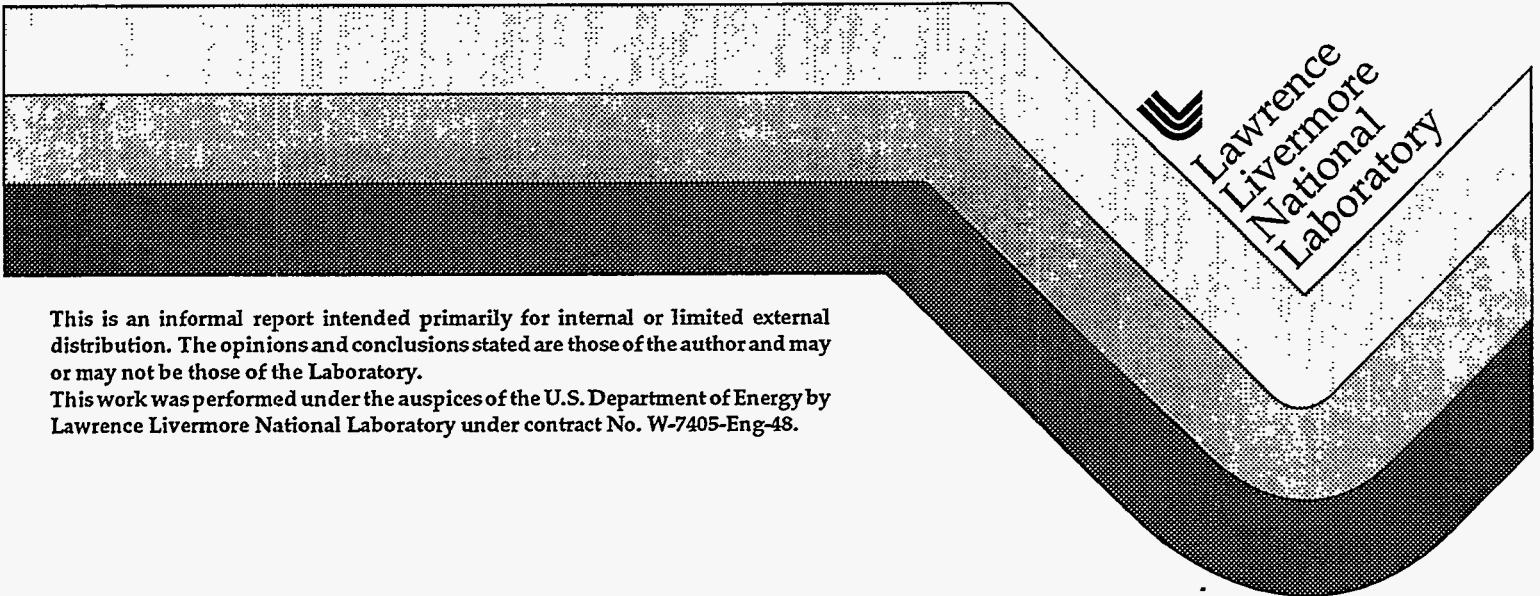
12
2-14-95 g s (1)

JEFFERSON

Containment Data Report

Ted Stubbs
Billy Hudson
Ray Heinle

December 1994



This is an informal report intended primarily for internal or limited external distribution. The opinions and conclusions stated are those of the author and may or may not be those of the Laboratory.

This work was performed under the auspices of the U.S. Department of Energy by Lawrence Livermore National Laboratory under contract No. W-7405-Eng-48.

MASTER

DL

DISCLAIMER

This document was prepared as an account of work sponsored by an agency of the United States Government. Neither the United States Government nor the University of California nor any of their employees, makes any warranty, express or implied, or assumes any legal liability or responsibility for the accuracy, completeness, or usefulness of any information, apparatus, product, or process disclosed, or represents that its use would not infringe privately owned rights. Reference herein to any specific commercial product, process, or service by trade name, trademark, manufacturer, or otherwise, does not necessarily constitute or imply its endorsement, recommendation, or favoring by the United States Government or the University of California. The views and opinions of authors expressed herein do not necessarily state or reflect those of the United States Government or the University of California, and shall not be used for advertising or product endorsement purposes.

This report has been reproduced
directly from the best available copy.

Available to DOE and DOE contractors from the
Office of Scientific and Technical Information
P.O. Box 62, Oak Ridge, TN 37831
Prices available from (615) 576-8401, FTS 626-8401

Available to the public from the
National Technical Information Service
U.S. Department of Commerce
5285 Port Royal Rd.,
Springfield, VA 22161

DISCLAIMER

Portions of this document may be illegible in electronic image products. Images are produced from the best available original document.

| <u>Classification Guide</u> | <u>Topic Number</u> | <u>Subject</u> |
|-----------------------------|---------------------|--|
| COK-88-024 | 1.5.6 | Event announcement |
| NV-89-18 | | Event announcement |
| TCG-WT-1 | 1113 | Contractor identification |
| TCG-WT-1 | 1121 | Personnel identification |
| TCG-WT-1 | 1210 | Geology |
| TVG-WT-1 | 1260 | Crater (map) |
| TCG-WT-1 | 1413 | Statement concerning venting |
| TCG-WT-1 | 1452 | Event announcement |
| TCG-WT-1 | 1831 | Depth of burial |
| TCG-WT-1 | 1843 | Stemming material, amount,etc |
| TCG-WT-1 | 1925 | Diagnostic canister dimensions |
| TCG-WT-1 | 3542.3 | Ground motion |
| TCG-WT-1 | 4810 | Radiation measurement |
| TCG-WT-1 | 4820 | Acceleration, pressure, temperature measurement |

DISTRIBUTION OF THIS DOCUMENT IS UNLIMITED

JEFFERSON Instrumentation Summary

| <u>Instrumentation</u> | <u>Fielded</u> | <u>Data Return</u> | <u>Present in this Report</u> |
|---------------------------|----------------|--------------------|-------------------------------|
| <u>Plug Placement</u> | yes | yes | yes |
| <u>Radiation</u> | yes | yes | yes |
| <u>Pressure</u> | | | |
| Stemming | yes | yes | yes |
| Challenge | no | - | - |
| Cavity | no | - | - |
| Atmospheric | no | - | - |
| <u>Motion</u> | | | |
| Free field | no | - | - |
| Surface | yes | yes | yes |
| Plug | no | - | - |
| Stemming | yes | yes | yes |
| Surface casing | no | - | - |
| Emplacement pipe | no | - | - |
| Recording trailer | yes | yes | yes |
| <u>Hydroyield (a)</u> | yes | yes | no |
| <u>Collapse (b)</u> | yes | yes | yes |
| <u>Stress (c)</u> | yes | yes | yes |
| <u>Strain (d)</u> | yes | yes | yes |
| <u>Other Measurements</u> | yes | yes | yes |

- (a) CORRTEX in emplacement hole.
- (b) EXCOR and CLIPER in emplacement hole.
- (c) In bottom plug.
- (d) In top plug.

Event Personnel

Containment Physics

| | |
|---------------|----------|
| B. Hudson | LLNL |
| J. Kalinowski | EG&G/AVO |
| T. Stubbs | EG&G/AVO |

Instrumentation

| | |
|--------------|----------|
| C. Cordill | LLNL |
| R. Salazar | EG&G/AVO |
| R. Spilsbury | EG&G/NVO |
| A. Moeller | EG&G/NVO |

1. Event Description

1.1 Containment summary

The JEFFERSON event was detonated in hole U20ai of the Nevada Test Site (see figure 1.1). Detonation time was 06:30 PDT on April 22, 1986. A subsurface collapse extending upward to a depth of about 190 m (just above plug four, the stemming platform) occurred about 2 hours 38 minutes after detonation. No radiation arrivals were detected above ground and the JEFFERSON event containment was considered satisfactory.

1.2 Site

A magnified geologic map showing some of the surface features near the U20ai site is shown in Figure 1.2. The device had a burial depth of 608 m in Area 4 tuffs, about 20 m above the static water level (SWL), as shown in the geologic cross sections (figure 1.3⁽¹⁾).

Stemming of the 2.44 m diameter emplacement hole followed the plan shown in figure 1.4. A log of the stemming operations was maintained by Holmes & Narver⁽²⁾.

1.3 Instrumentation

Figure 1.5 gives a schematic layout of the instrumentation in hole U20ai, designed to monitor the stemming emplacement procedures and performance on the JEFFERSON event.

Each of the five sanded gypsum concrete (SGC) plugs was monitored during emplacement with arrays of thermistors and conductivity probes to determine its position, thickness and curing history. Pressure and radiation were monitored in the coarse stemming on either side of the central three SGC plugs. All data signals from these stations were transmitted in analog form to the recording trailer where they were recorded on magnetic tape.

Sensitive pressure transducers were fielded below plugs 4 & 5 and in the ground surface as part of an investigation of the permeability of the upper layers of the Nevada Test Site. Signals from these stations were digitized through a Waveteck[®] system and recorded on disk by a LSI 11/23 computer.

Hydrodynamic yield of the device and cavity collapse and chimney formation were monitored by two CLIPER/CORRTEX cables and one EXCOR/CORRTEX cable. Results of the hydrodynamic yield measurements are reported elsewhere⁽³⁾.

BI-axial stress and strain transducers⁽⁴⁾ were fielded in the bottom plug as part of a continuing transducer development program to measure stress near the 1.0 Kbar level.

Vertical motion was monitored in each of the five SGC plugs, in the stemming between the plugs, on the surface casing and in the ground surface, 15.24 m from surface ground zero (SGZ). Triaxial motion of the recording trailer was also recorded. Relative displacement between the surface casing and the top plug was monitored by an array of seven proximity switches mounted in the plug next to the bottom of the surface casing.

A brief history of the fielding operations of the instrumentation, including emplacement pipe strain measurements, is given in reference 5. Further details of the instrumentation are given in reference 6.

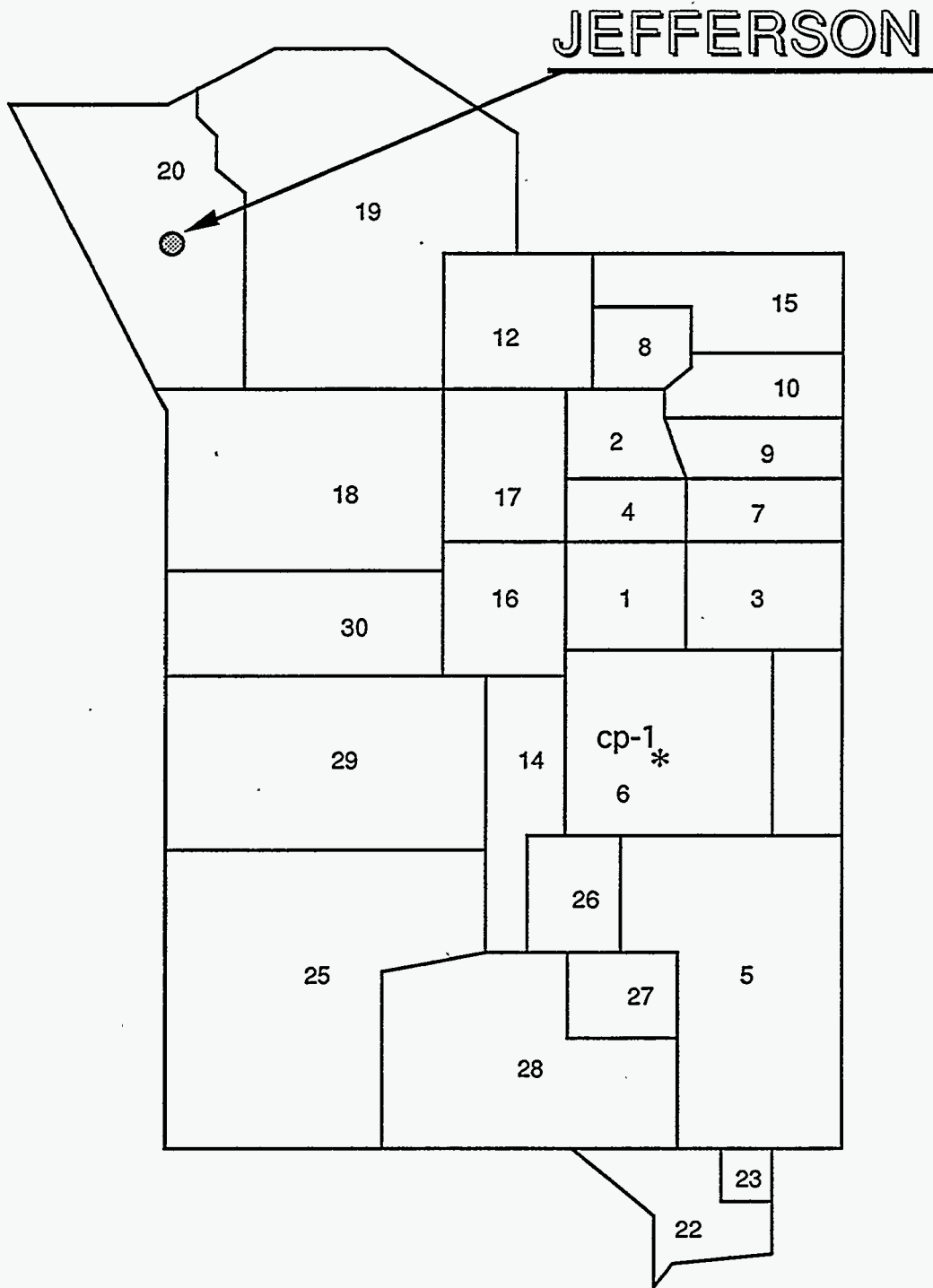


Figure 1.1 Map of the Nevada Test Site indicating the location of hole U20ai.

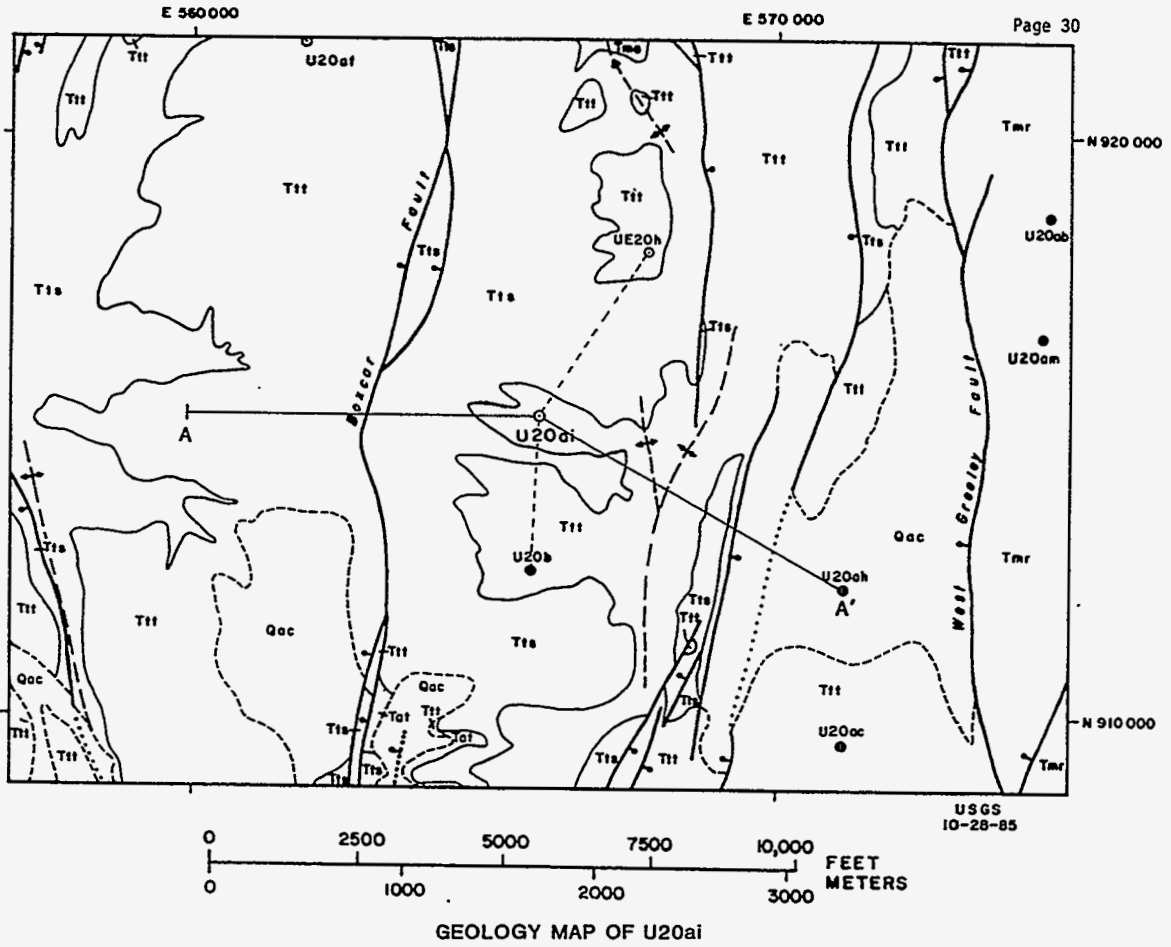
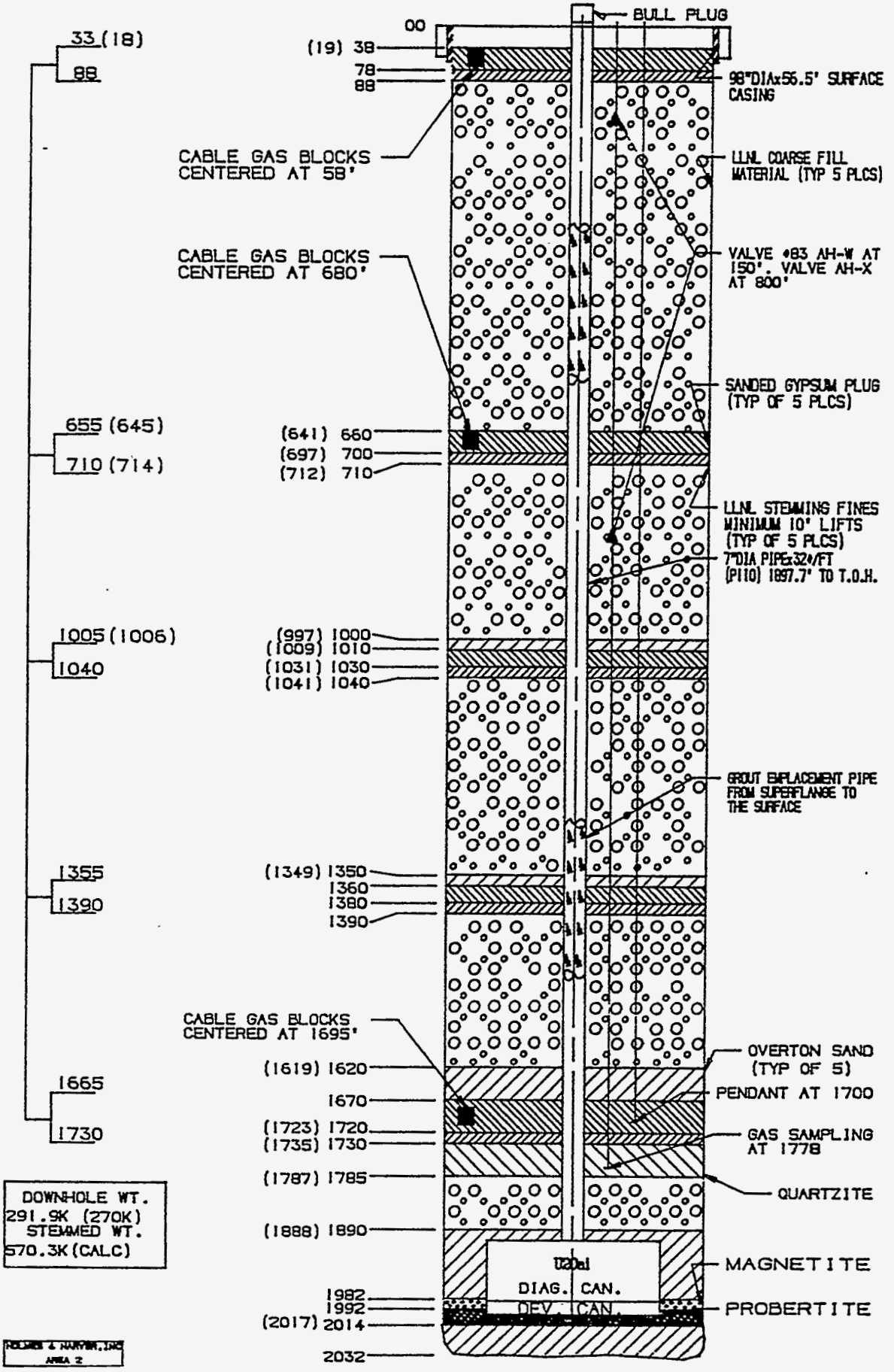


Figure 1.2 Geologic Map of the region near hole U20ai.

J E F F E R S O N U 2 0 a i



DOWN-HOLE WT.
291.9K (270K)
STEMMED WT.
570.3K (CALC)

POULSEN & HARTMAN, INC
AREA 2

Figure 1.4 As-built stemming plan for hole U20ai.

AS-BUILT CONFIGURATION

U20ai

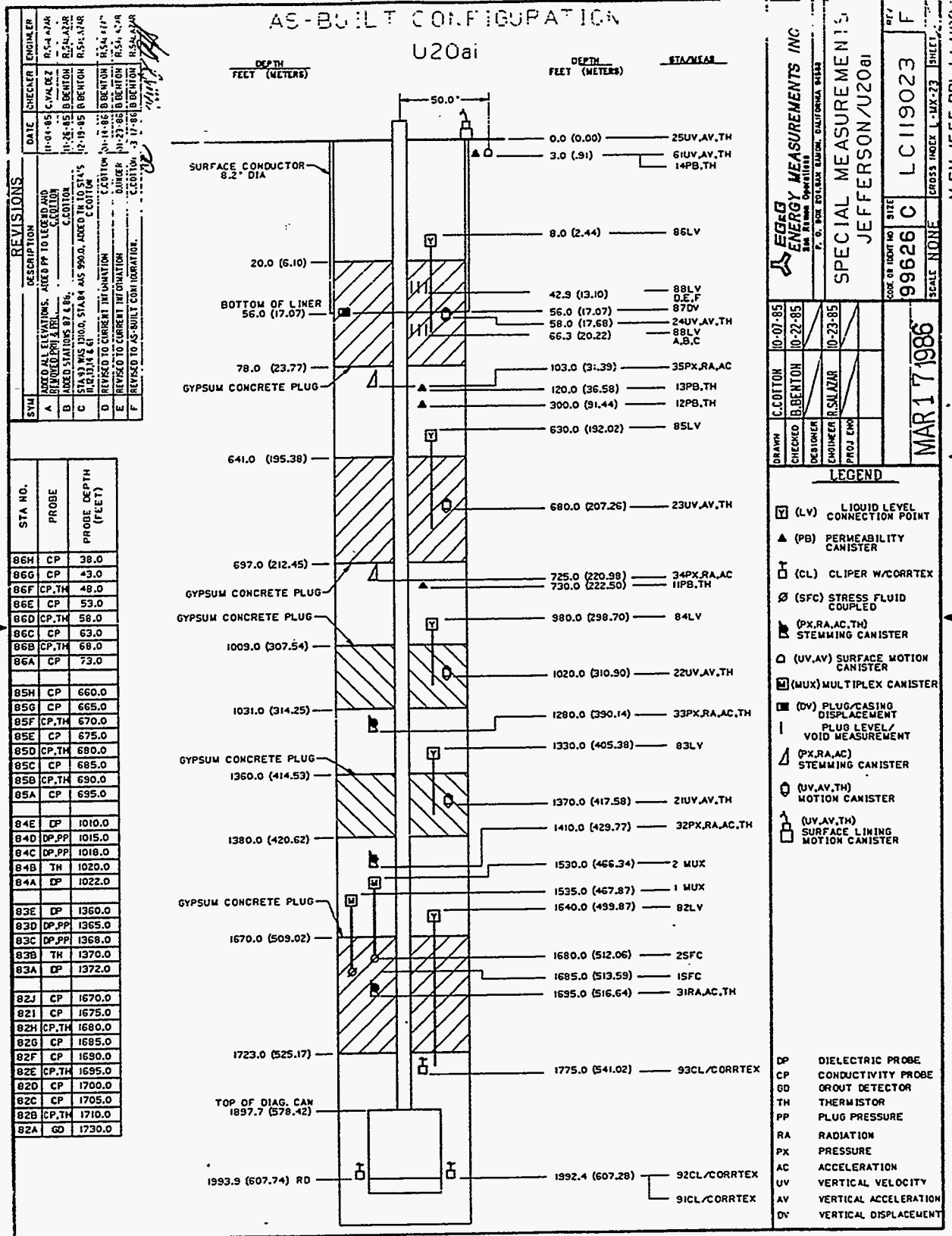


Figure 1.5 As-built containment instrumentation plan for the JEFFERSON event emplacement hole U20ai.

2. Emplacement

2.1 Instrumentation

During installation, some of the mounting brackets were broken on the motion canisters intended to be placed in plugs one, three and four. This allowed the orientation of the canisters to be slightly off vertical.

2.2 Pipe strain

Strain on the emplacement pipe was not recorded on JEFFERSON.

2.3 Plug levels and temperature

The emplacement of each of the five SGC plugs was monitored with an array of conductivity probes and thermistors. The locations of the probes are tabulated in figure 1.5. Figures 2.1-2.5 show plots of the SGC emplacement and temperature histories. Open circles indicate the upper and lower boundary positions of the plugs as measured using tag lines while solid circles indicate the positions of the probe stations and the times at which the conductivity probes were activated. Most of the temperature sensors accompanied conductivity probes as indicated in figure 1.5 and the captions of figures 2.1–2.5. The temperature probes in the second and third plugs were fielded midway between conductivity sensors.

All plugs were emplaced as planned.

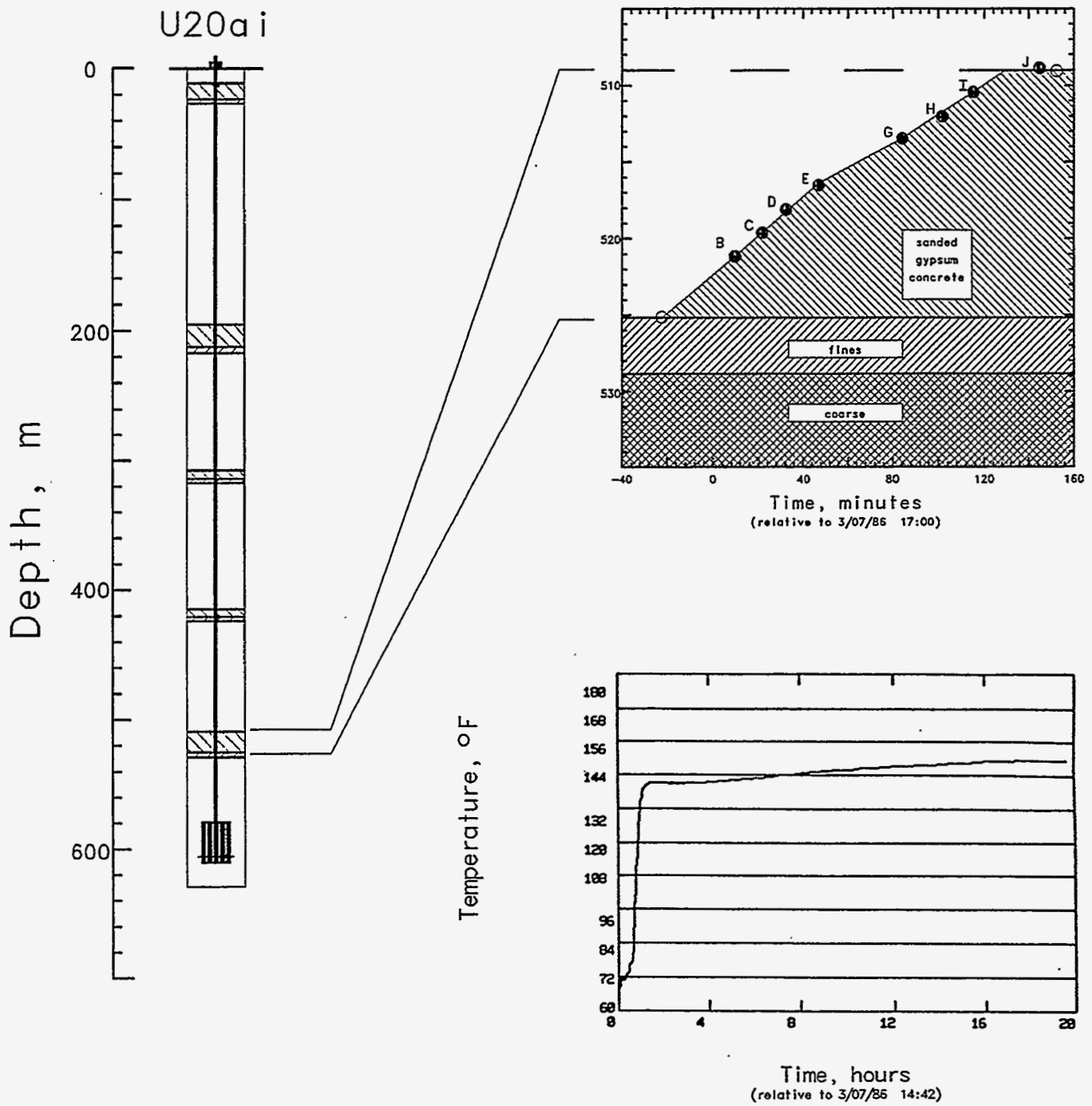


Figure 2.1 Sanded gypsum emplacement for the first plug. The upper and lower plug boundaries were determined with a tag line (open circles). Solid symbols indicate the probe elevations. Probes labeled B, E, and H included temperature sensors. The temperature history of probe B is shown as representative of the first 20 hours.

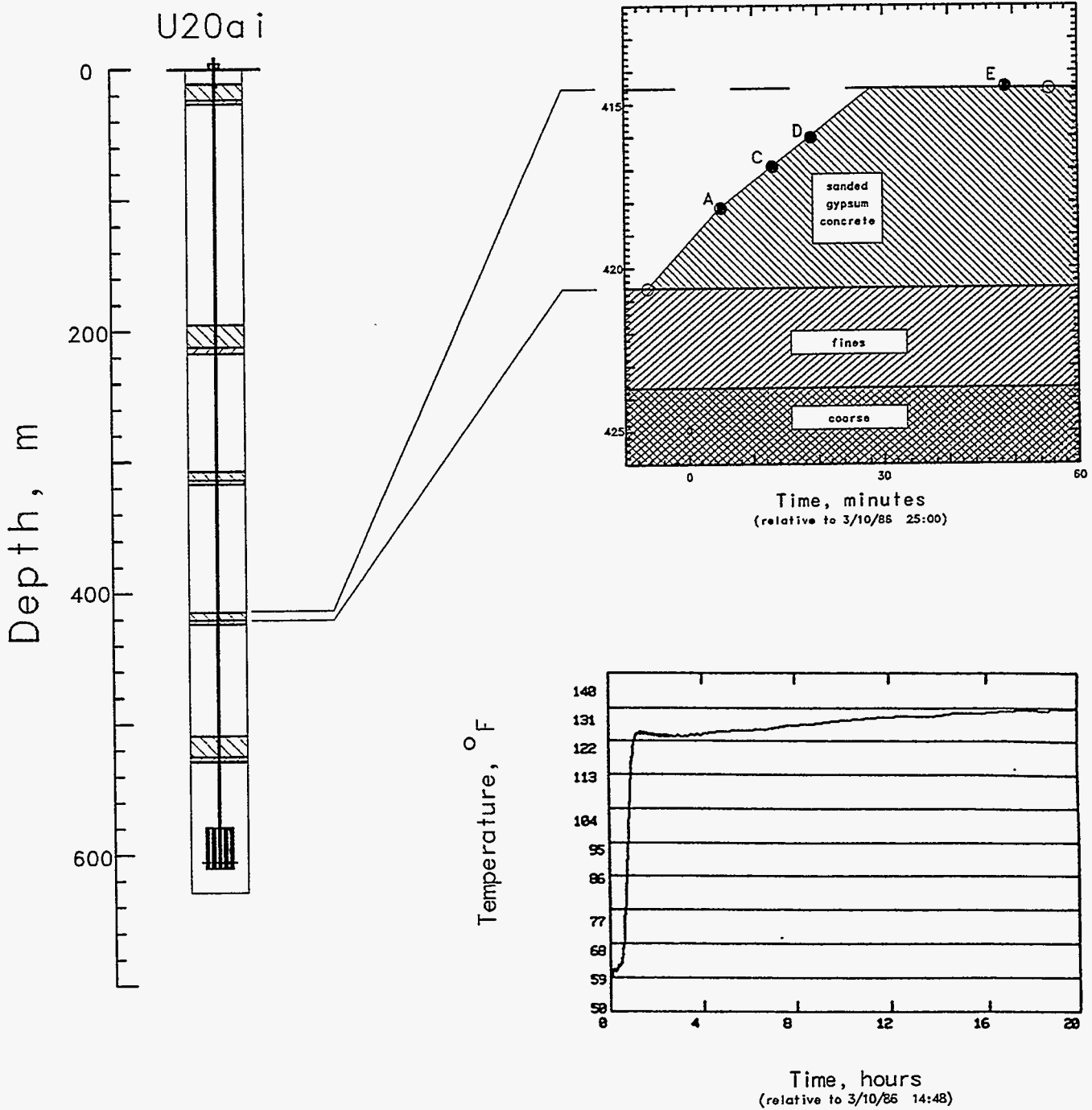


Figure 2.2 Sanded gypsum emplacement for the second plug . The upper and lower plug boundaries were determined with a tag line (open circles). Solid symbols indicate the probe elevations. Probe labeled B included only a temperature sensor and is not shown in the grout level plot. It was located midway between probes A and C.

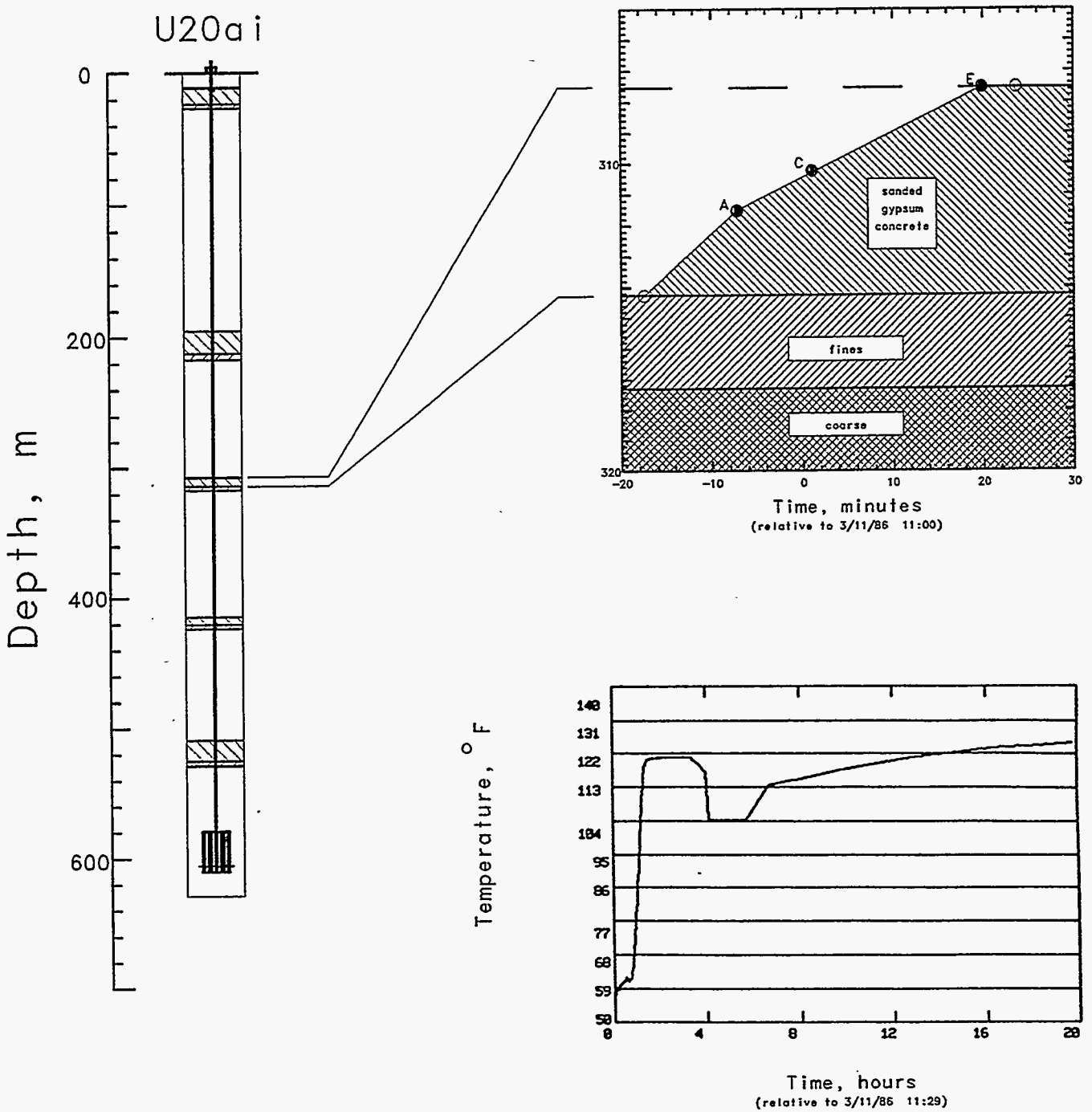


Figure 2.3 Sanded gypsum emplacement for the third plug. The upper and lower plug boundaries were determined with a tag line (open circles). Solid symbols indicate the probe elevations. Probe labeled B included a only temperature sensor and is not shown in the grout level plot. It was located midway between probes A and C. The dip in temperature near the four-hour point of the record is due to grouting of the emplacement pipe.

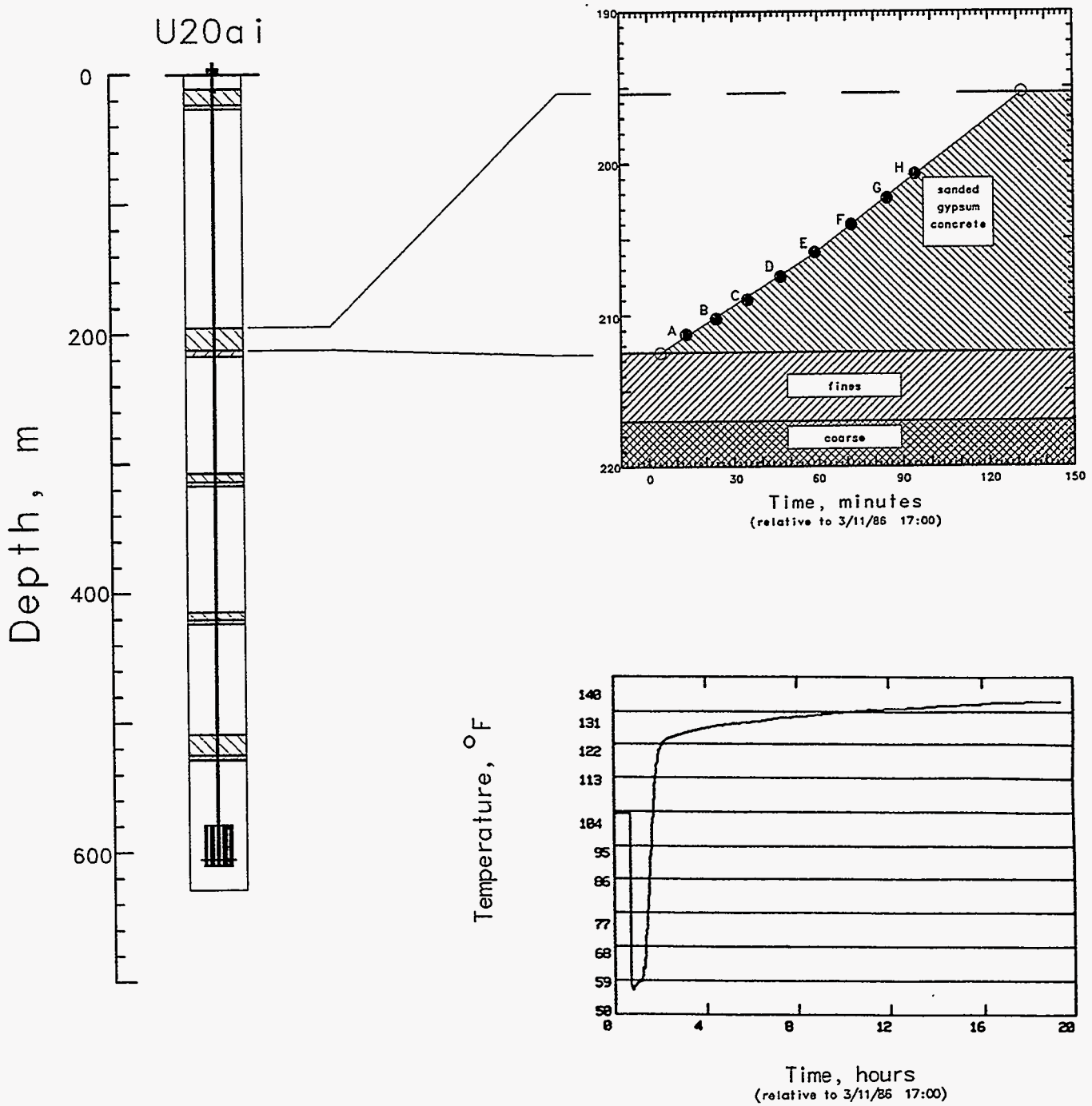


Figure 2.4 Sanded gypsum emplacement for the fourth plug. The upper and lower plug boundaries were determined with a tag line (open circles). Solid symbols indicate the probe elevations. Probes labeled B, D, and F included temperature sensors. The temperature history of probe F is shown as representative of the first 20 hours. The initial temperature level (about 104 degrees F) is unexplained.

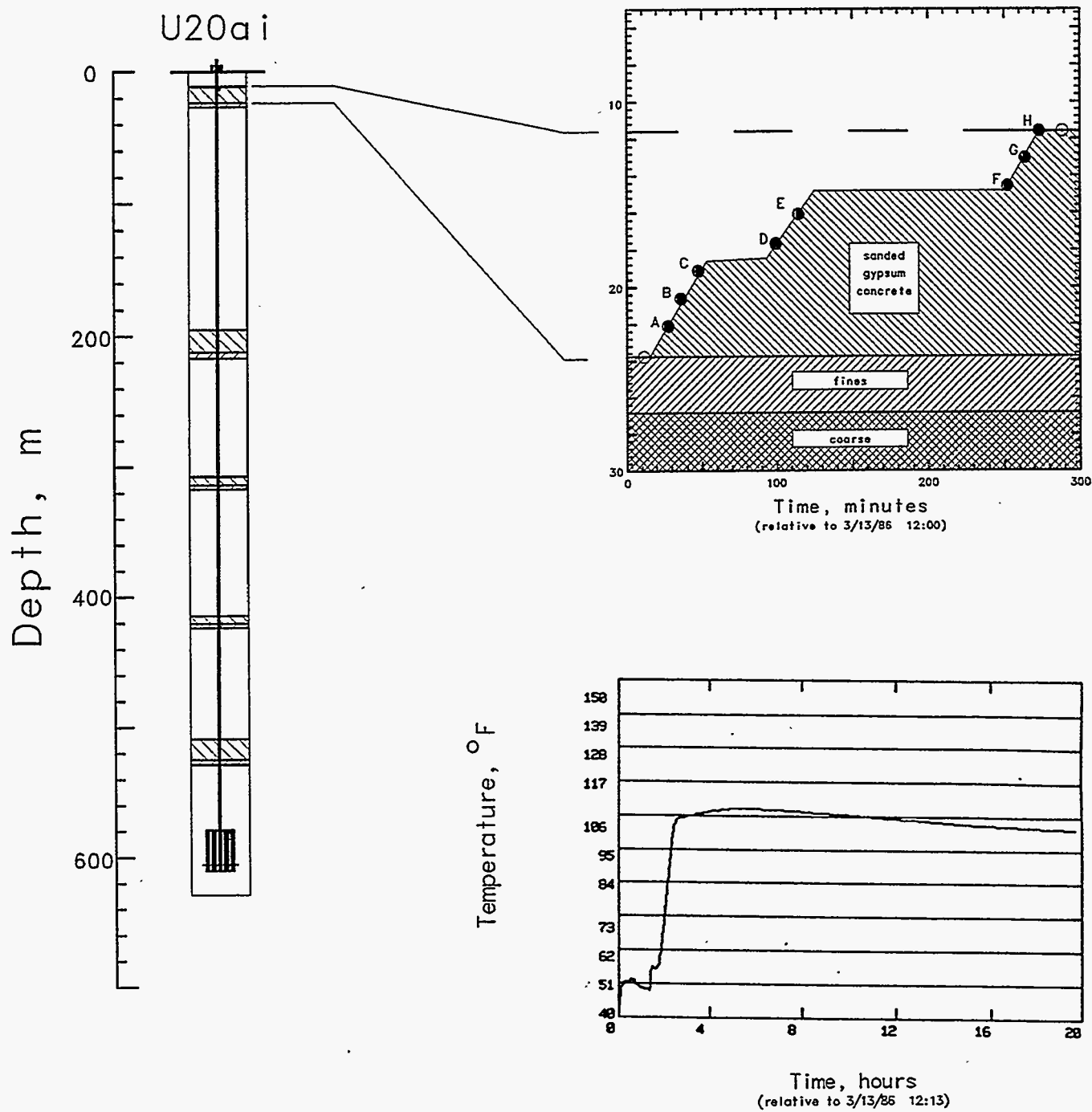


Figure 2.5 Sanded gypsum emplacement for the fifth plug . The upper and lower plug boundaries were determined with a tag line (open circles). Solid symbols indicate the probe elevations. Probes labeled B, D, and F included temperature sensors. The temperature history of probe D is shown as representative of the first 20 hours.

3. Stemming Performance

All signals from stations at depths greater than 31 m in the emplacement hole were lost at about 2 s after detonation. This loss was most likely due to cable breakage caused by the excessive motion associated with the explosion. All recording was terminated 32 hours after the detonation.

3.1 Radiation and Pressure

As indicated in Figure 1.4, pressure and radiation were monitored in the region below each of the upper four SGC plugs.

Pressure and radiation histories, from a few seconds before detonation until recording termination or station failure, are displayed in Figures 3.1–3.5. The radiation signal from station 31 (in the bottom plug) went beyond band edge prior to 2 s while stations at shallower depths show little, if any, indication of radiation arrivals. At station 32 (below the second SGC plug) a large pressure pulse arrives at about 0.1 s and peaks at about 0.5 s with a pressure change of around 22 psi. Stations at shallower depths show a different behavior, suggesting that the early time pressure history of the stemming column may be that of compaction and dilatation due to the passage of the shock wave.

All pressure and radiation data are consistent with satisfactory containment.

3.2 Motion

Recording on magnetic tapes containing the data from all stations in the SGC plugs (except station 31), the ground surface and on the surface casing was halted at about 2 s by the strong explosion-induced motion of the recording trailer. Stations 24 (in the top plug), 25 (on the surface casing), and 35 (in the stemming below the top plug) were the only stations in the emplacement hole to survive beyond 2.5 seconds. Although station 24 and 25 survived, the tapes recording the signals were halted at that time precluding further explosion-induced motion from these stations. Subsequently, the tapes were restarted manually when the field crew re-entered the trailer.

Figures 3.6–3.16 show the explosion-induced vertical acceleration measured in the coarse stemming and in the stemming plugs. Station 25 monitored the vertical acceleration and velocity of the surface casing while station 61 monitored the vertical motion of the ground surface at a depth of 0.91 m and a horizontal range of 15.24 m from SGZ. Characteristics of the motion and motion transducers are given in tables 3.1–3.3.

3.3 Collapse

All three of the EXCOR cables were active post-shot. The time variation of the position of the deepest end of the cables as a function of time is shown in Figure 3.17. Subsurface collapse appears to have progressed upwards to a depth of about 190 m (close to the top of the fourth plug). A slight increase in pressure (about 0.1 psi) was registered at station 35 at about 9485 s and is plotted in figure 3.17 as a circle. The acceleration history of station 35 is superimposed (without amplitude scale) on figure 3.17 at the approximate elevation of that station. The acceleration seen corresponds to the collapse history reported by the EXCOR and suggests that the pressure change is the result of a slight stemming shift and that the stemming remains otherwise in place below the top plug.

The motion sensed at stations 24, 35, and 61 during the collapse phase (about 2 hours and 38 minutes) was of too low a magnitude to be meaningfully integrated, so only the measured signals are shown. The proximity switch array (station 87) registered no change of relative position of the top plug and surface casing at any time and the data from this station are not shown.

Table 3.1 Summary of Motion

| Gauge | Slant Range (m) | Arrival Time (ms) | Peak Acceleration (g) | Peak Velocity (m/s) | Peak Displacement (m) | Residual Displacement (cm) |
|-------|-----------------|-------------------|-----------------------|---------------------|-----------------------|----------------------------|
| 21av | 190 | 74 | 22.4, 48.0 | 21.2 | 5.3 | (a) |
| 21uv | | - | - | 20.7 | 4.3 | (a) |
| 22av | 297 | 115 | 8.0, 3.6 | 5.8 | 2.1 | (a) |
| 22uv | | - | - | 5.7 | 2.0 | (a) |
| 23av | 401 | 160 | 2.2, 1.0 | 3.6 | 1.02 | (a) |
| 23uv | | (b) | - | - | - | - |
| 24av | 590 | 139(c), 288 | 3.54, 8.3(d) | 5.1 | 2.65 | (a) |
| 24uv | | - | - | 4.9 | 2.45 | (a) |
| 25av | 608 | 143(c), 296 | 4.1, 8(d) | 5.7 | 2.60 | (a) |
| 25uv | | - | - | 4.7 | 2.31 | (a) |
| 31av | 91 | 31(c), 41(e) | (a) | - | - | - |
| 32av | 142 | 41(c), 75 | 53 | 23.5 | 14.3(f) | (a) |
| 33av | 218 | 52(c), 83 | 8 | 7.8 | 3.4 | |
| 34av | 387 | 93(c), 156 | 4.4 | 5.0 | 2.3 | |
| 35uv | 577 | 139(c), 230 | 5.1(g), 24(d) | 5.1 | 2.56 | -34 |
| 61av | 608 | 310 | 5.0, 9.8(d) | 5.0 | 2.58 | (a) |
| 61uv | | - | - | 5.0 | 2.50 | (a) |

- (a) Signal lost before this value could be attained.
- (b) Channel lost before this datum was attained.
- (c) Emplacement pipe- or strongback-stemming interaction.
- (d) Slap-down peak.
- (e) Signal was lost at ground motion arrival.
- (f) Peak of displacement not reached.

Table 3.2 Accelerometer Characteristics

| Gauge | Natural Frequency (Hz) | Damping Ratio | System Range (g's) |
|---------|------------------------|---------------|--------------------|
| 21av | 1020 | 0.65 | 600 |
| 22av | 880 | 0.65 | 200 |
| 23av | 300 | 0.85 | 50 |
| 24av | 275 | 0.80 | 20 |
| 25av | 290 | 0.75 | 20 |
| 31av(a) | 30,000 | 0.002 | 5000 |
| 32av(a) | NA | NA | 500 |
| 33av(a) | NA | NA | 250 |
| 34av(a) | 2500 | 0.7 | 25 |
| 35av(a) | 2500 | 0.7 | 25 |
| 61av | 590 | 0.65 | 36 |

(a) manufacturer specifications

Table 3.3 Velocimeter Characteristics

| Gauge | Natural Frequency (Hz) | Time to 0.5 Amplitude (s) | Calibration Temperature (°C) | Operate Temperature (°C) | System Range (m/s) |
|-------|------------------------|---------------------------|------------------------------|--------------------------|--------------------|
| 21uv | 3.823 | 30.37 | 26.93 | 28.03 | 60 |
| 22uv | 4.068 | 18.51 | 26.12 | 23.01 | 32 |
| 23uv | 3.308 | 14.18 | 26.62 | 23.67 | 20 |
| 24uv | 3.463 | 9.76 | 26.57 | 21.97 | 12 |
| 25uv | 3.619 | 8.80 | 26.51 | 10.47 | 12 |
| 61uv | 3.553 | 9.46 | 24.76 | 8.41 | 12 |

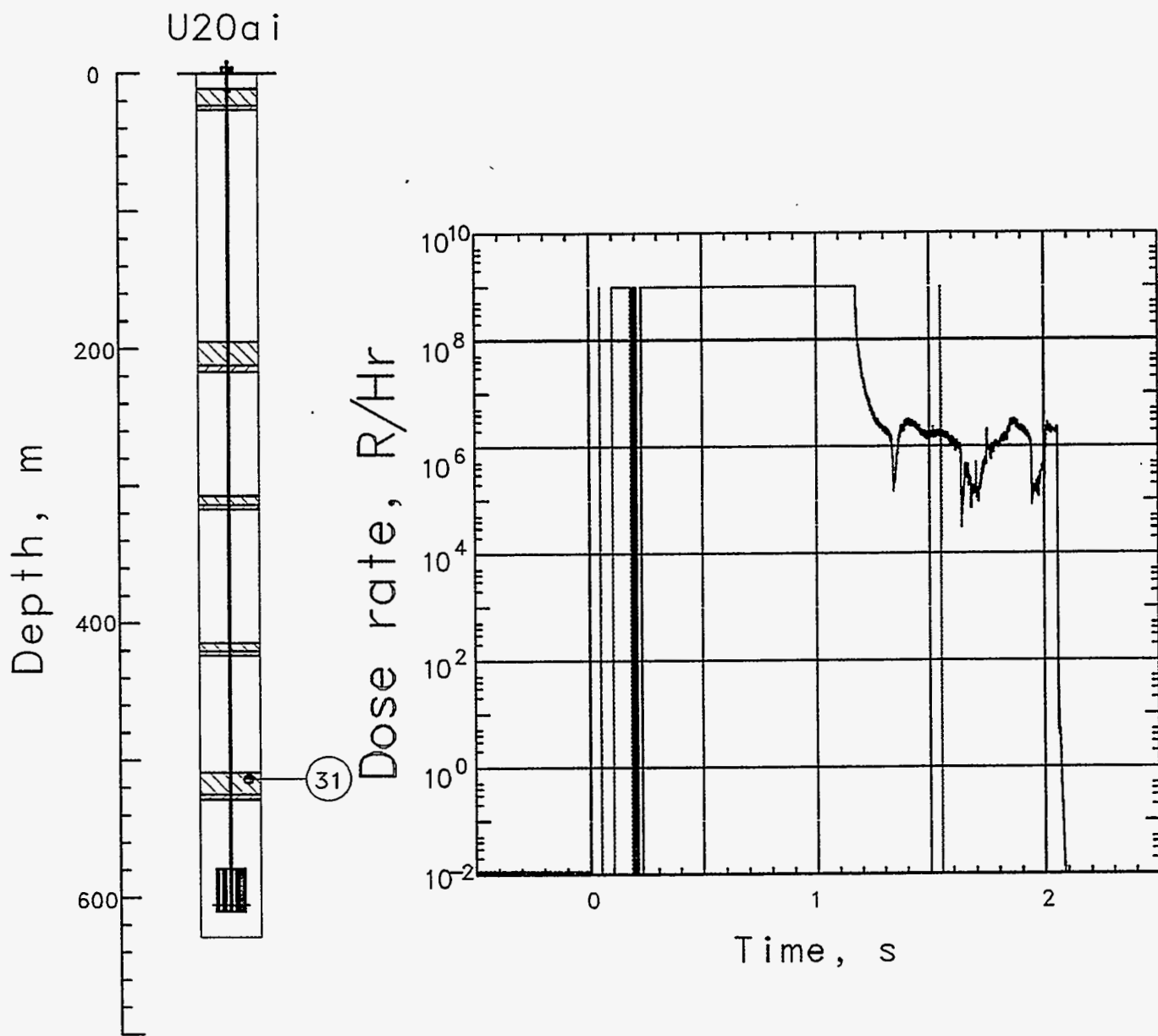


Figure 3.1 Radiation measured in the first SGC plug (station 31 at 516.6 m depth). Station signals were lost at about 2 s after detonation. There was no pressure transducer installed at this station.

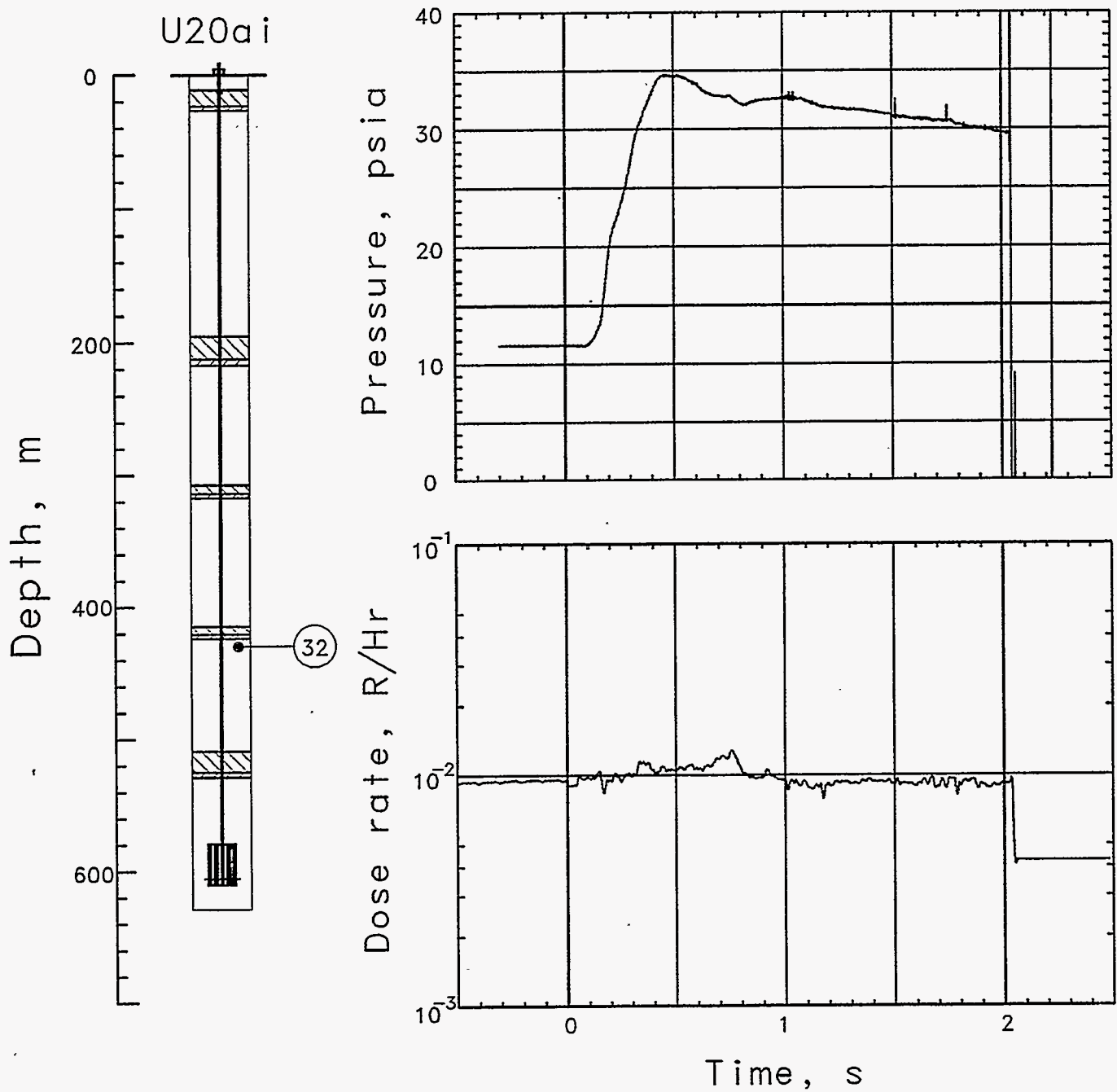


Figure 3.2 Pressure and radiation measured in the course stemming below the second SGC plug (station 32 at 466.3 m depth). Station signals were lost at about 2.1 s after detonation.

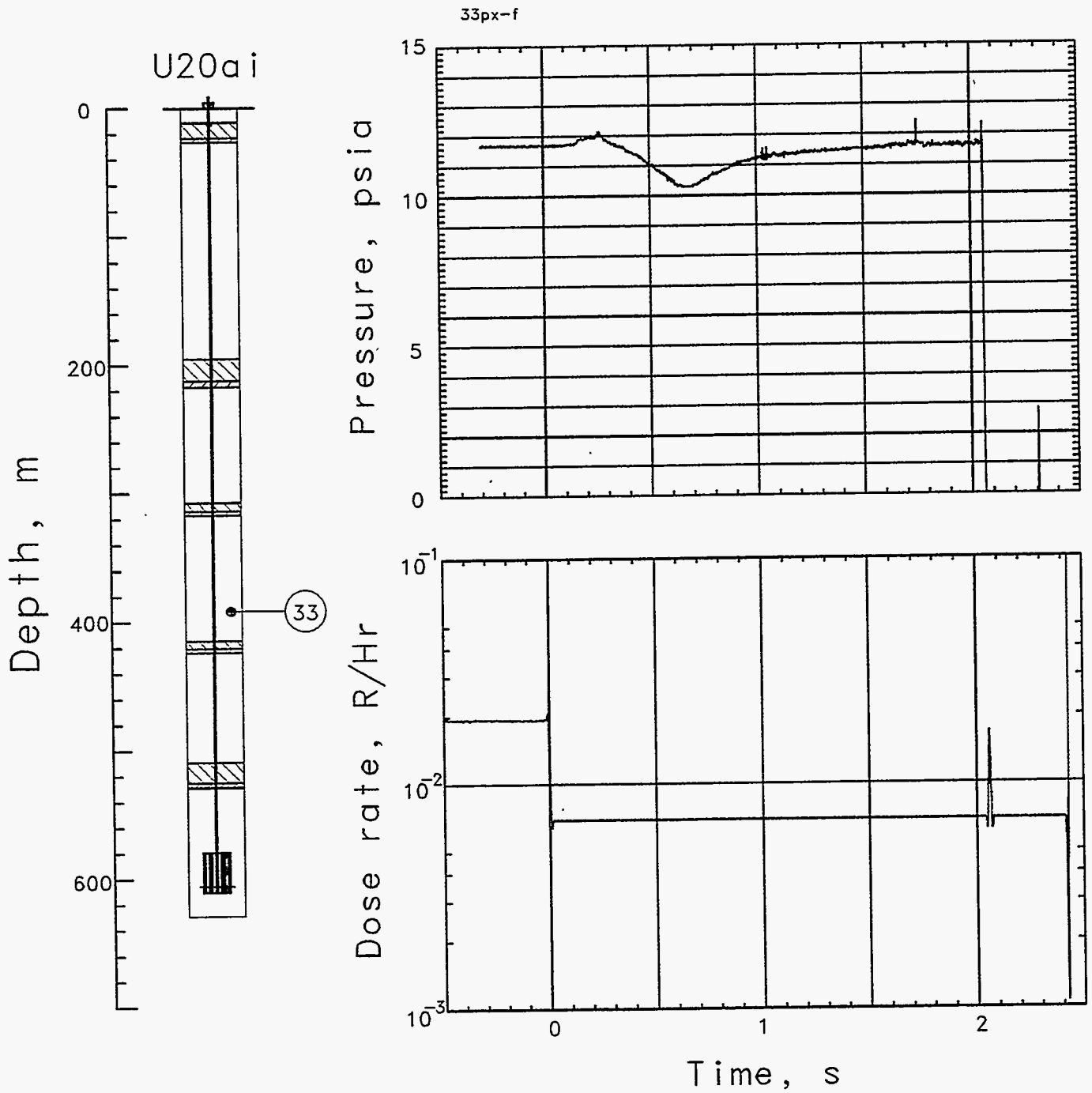


Figure 3.3 Pressure and radiation measured in the coarse stemming below the third SGC plug (station 33 at 390.1 m depth). Station signals were lost at about 2.1 s after detonation.

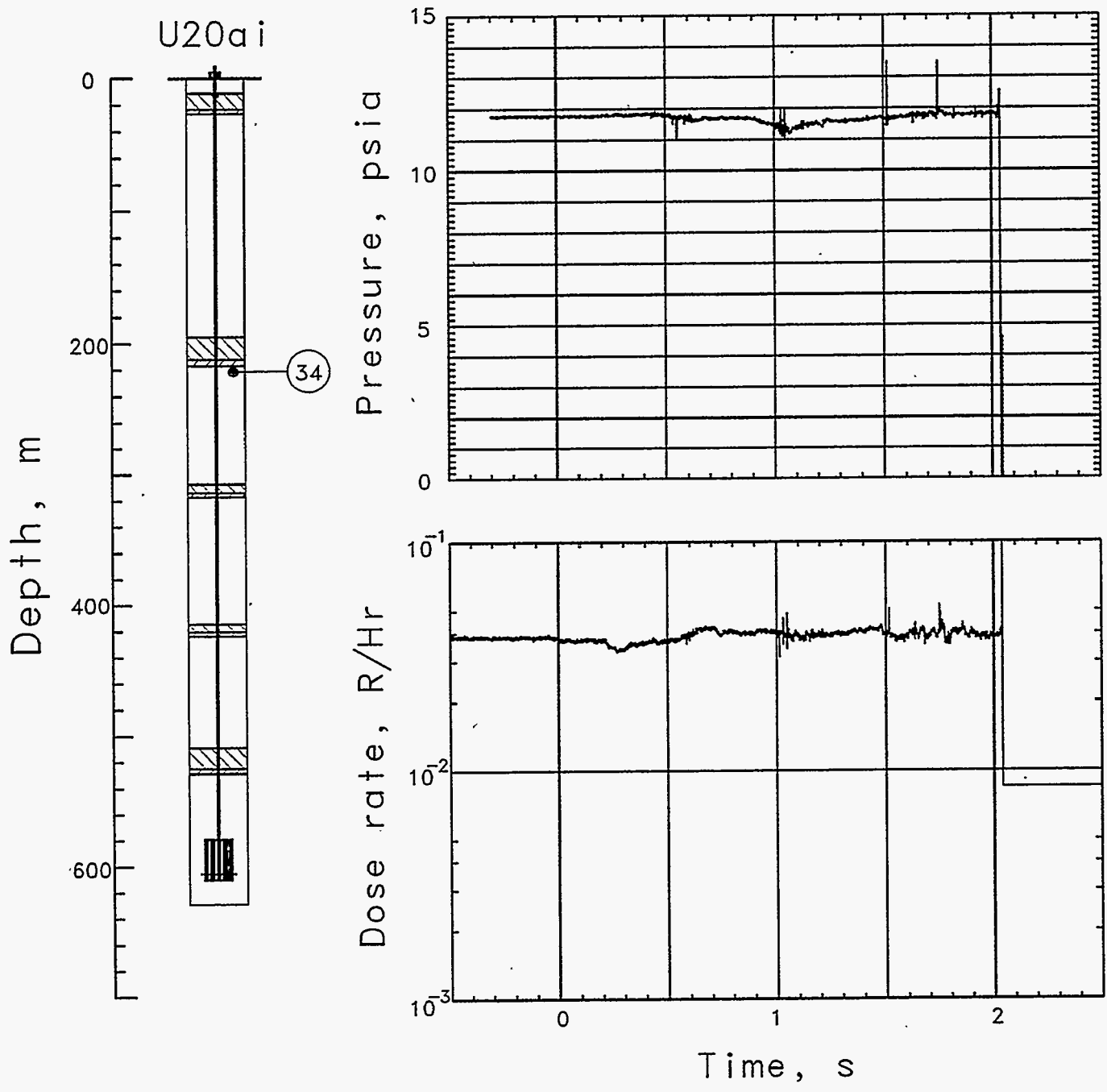


Figure 3.4 Pressure and radiation measured in the coarse stemming below the fourth SGC plug (station 34 at 221.0 m depth). Station signals were lost at about 2.1 s after detonation.

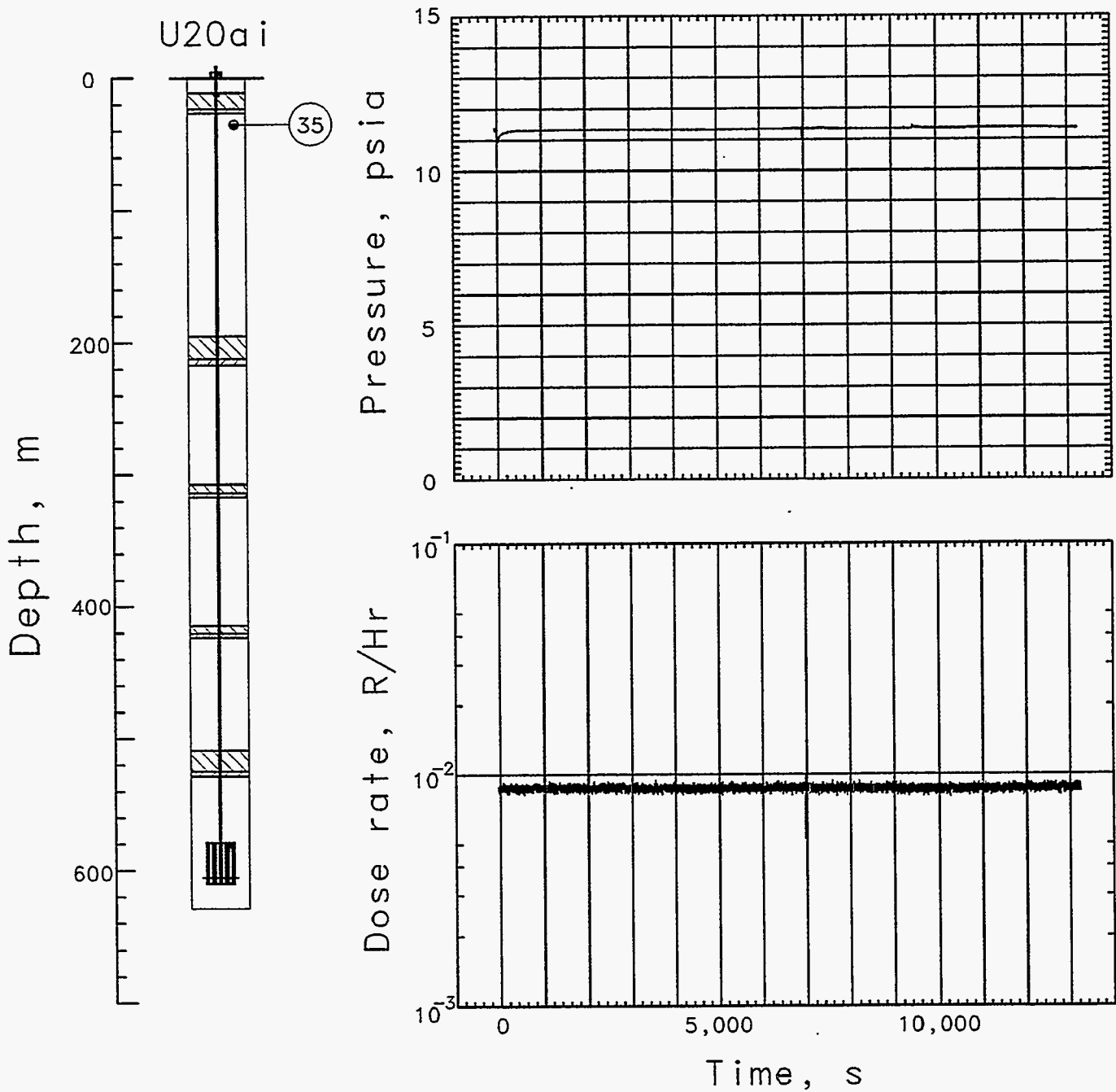


Figure 3.5 Pressure and radiation measured in the coarse stemming below the fifth SGC plug (station 35 at 31.4 m depth). The pressure drop at zero time is due to shock-induced ground motion and the jump in pressure at about 9500 s is associated with the subsurface collapse.

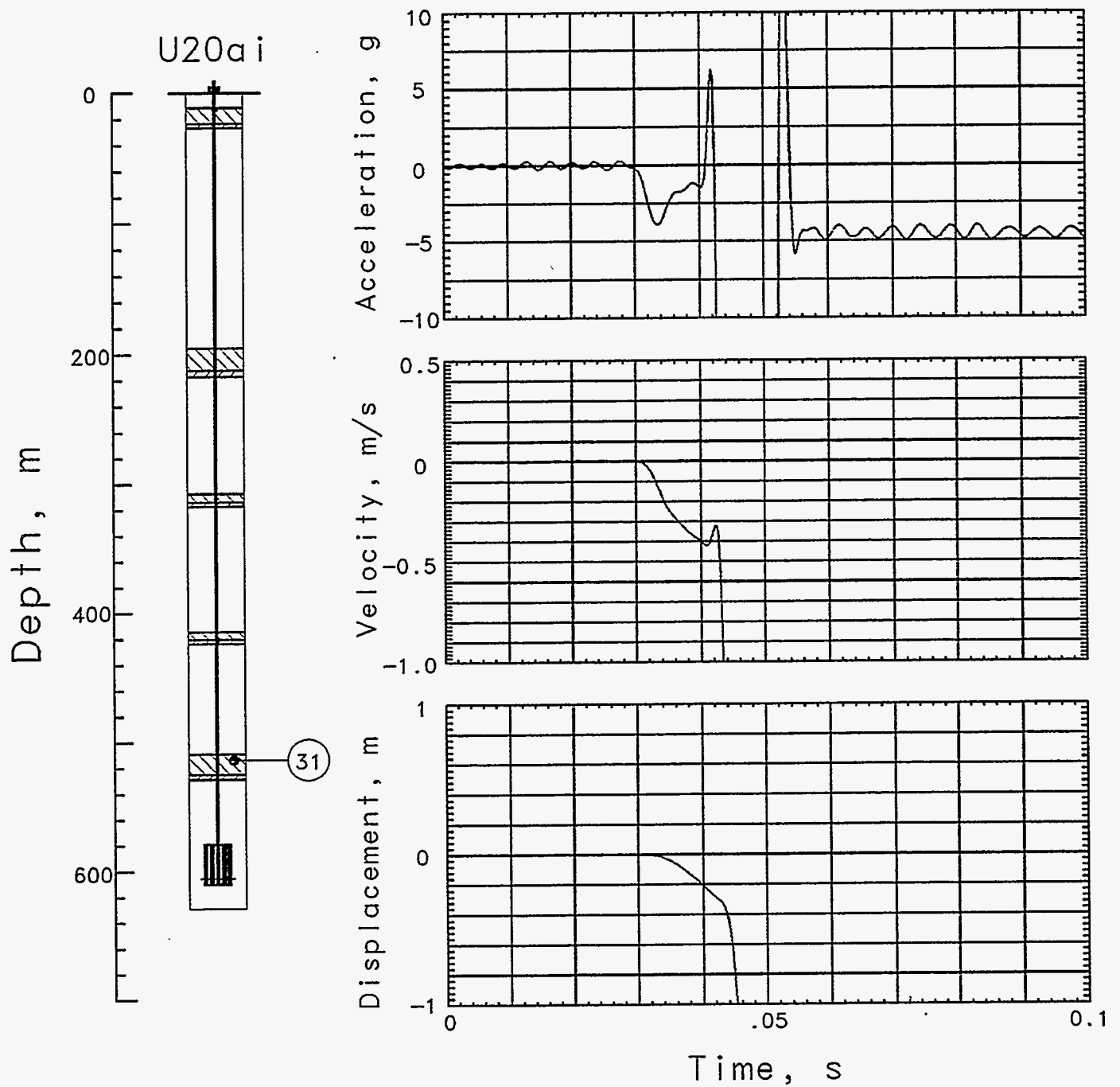


Figure 3.6 Explosion-induced vertical motion of the bottom plug at a depth of 516.6 m (station 31). The data are invalid after 42 ms. The anomalous negative-going initial motion is unexplained.

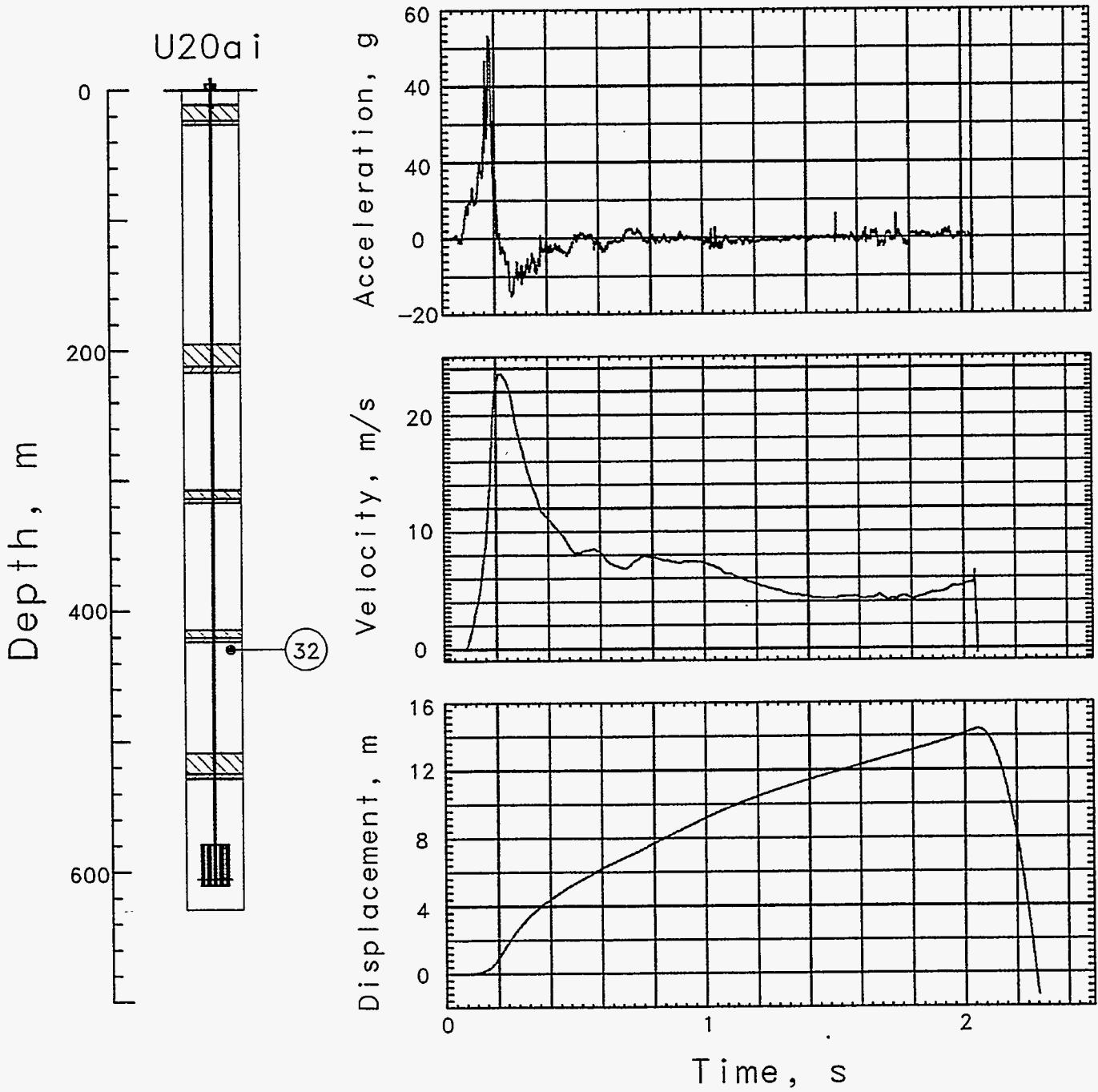


Figure 3.7 Explosion-induced vertical motion in the coarse stemming of the emplacement hole at a depth of 466.3 m (station 32). Station signals were lost at about 2.1 s after detonation.

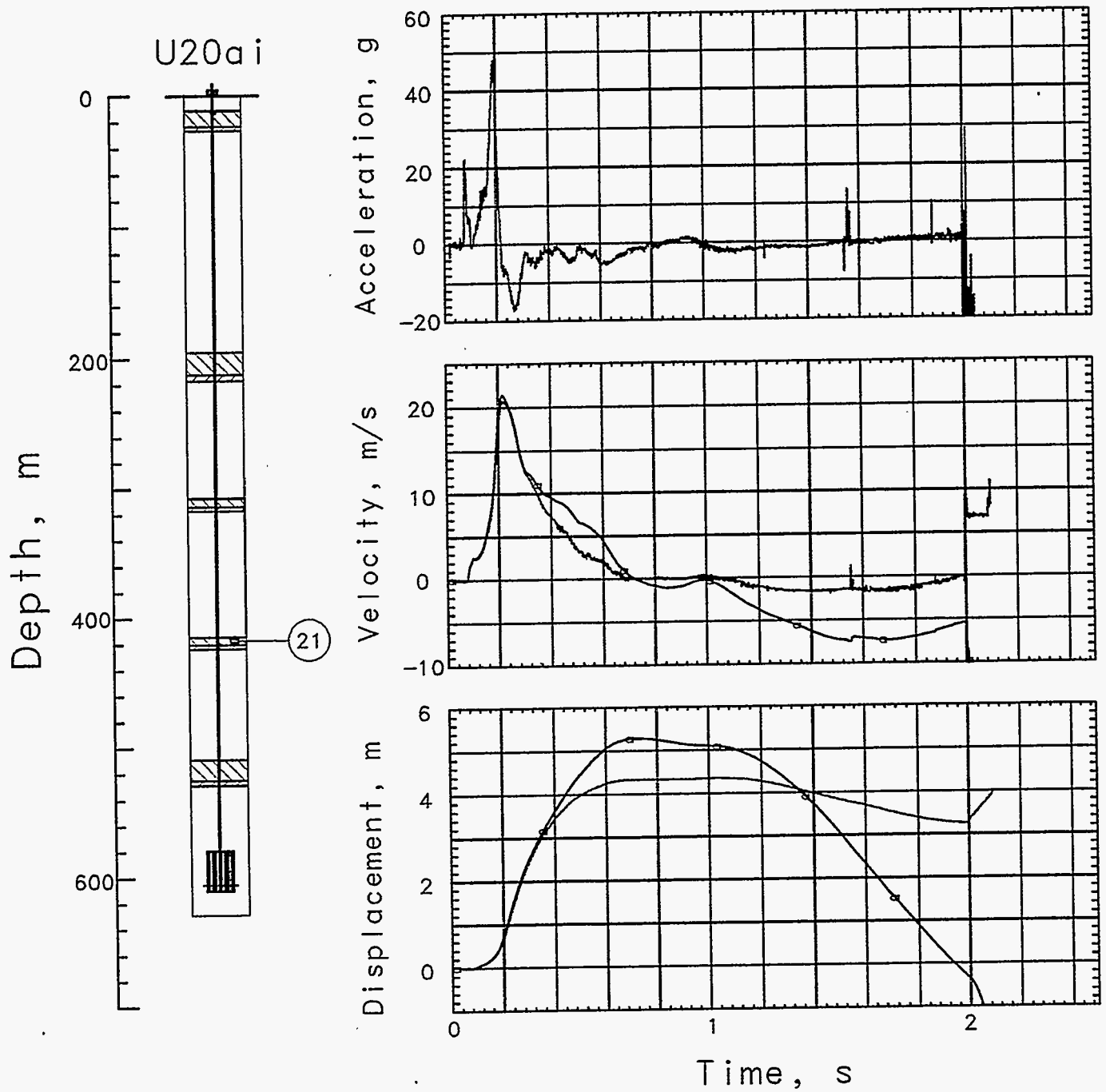


Figure 3.8 Explosion-induced vertical motion of the second plug at a depth of 417.6 m (station 21). Station signals were lost at about 2.0 s after detonation. Data records annotated with an "a" were obtained from an accelerometer.

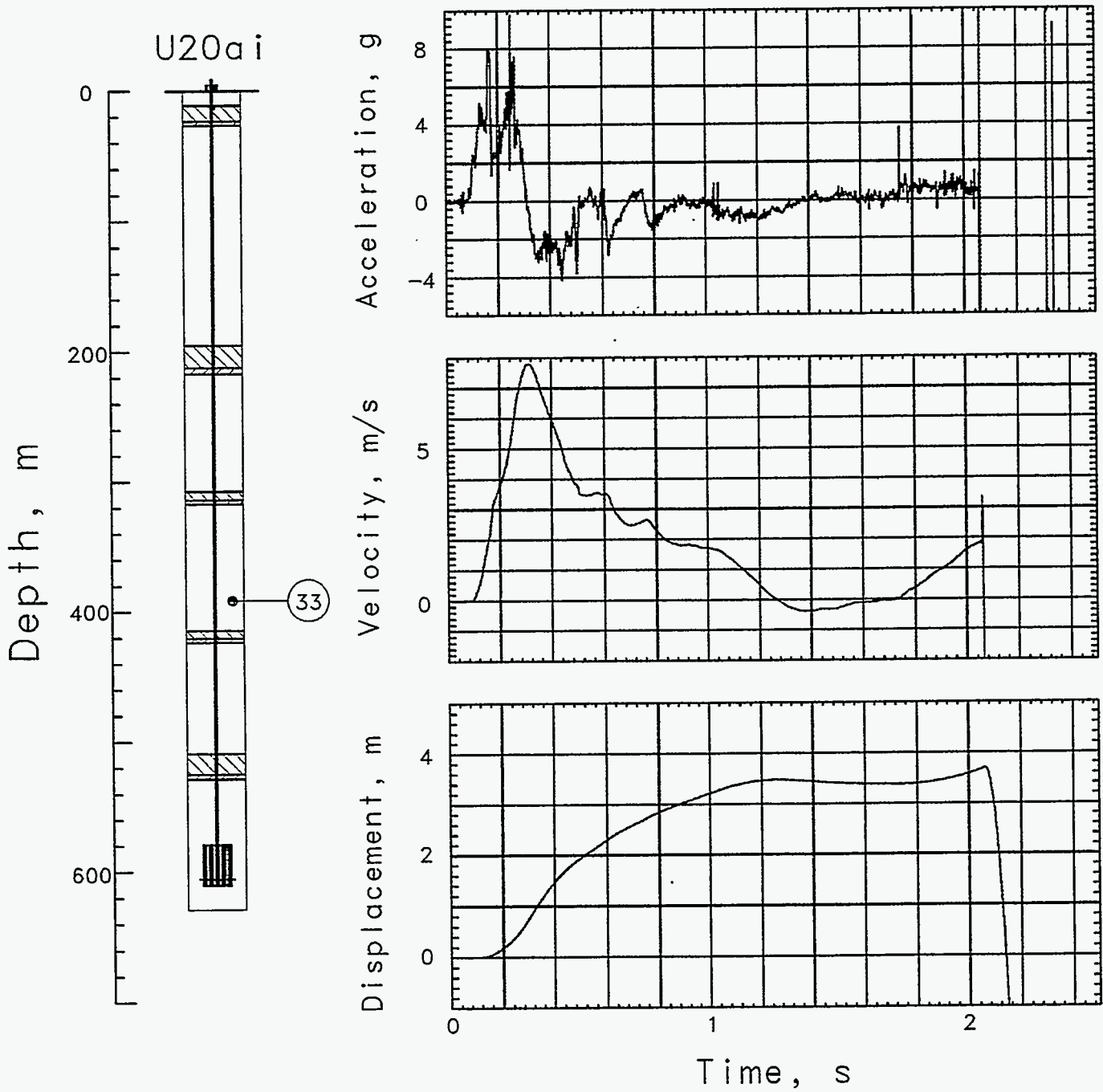


Figure 3.9 Explosion-induced vertical motion in the coarse stemming of the emplacement hole at a depth of 390.1 m (station 33). Station signals were lost at about 2.1 s after detonation.

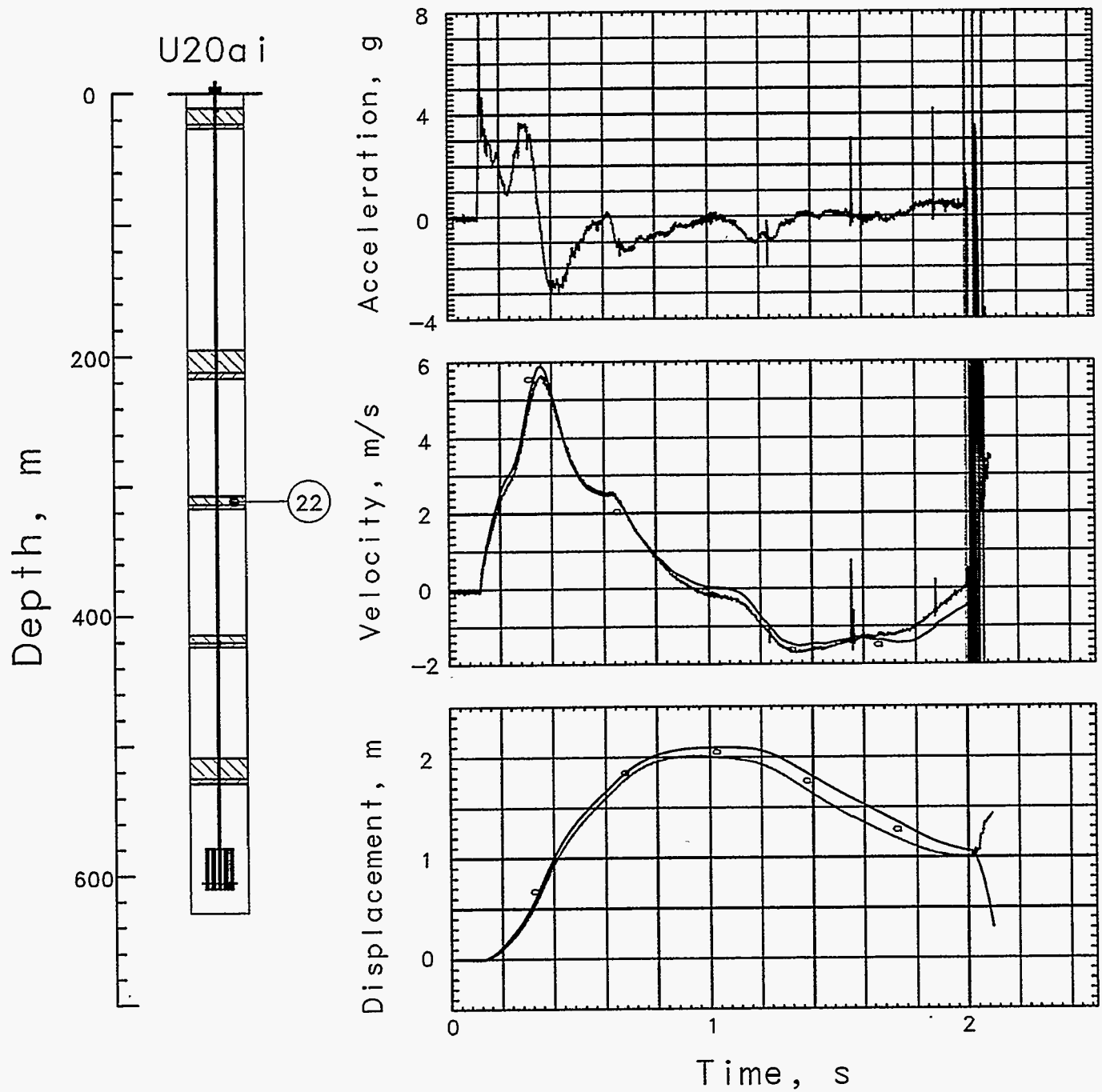


Figure 3.10 Explosion-induced vertical motion of the third plug at a depth of 310.9 m (station 22). Station signals were lost at about 2.0 s after detonation. Data records annotated with an "a" were obtained from an accelerometer.

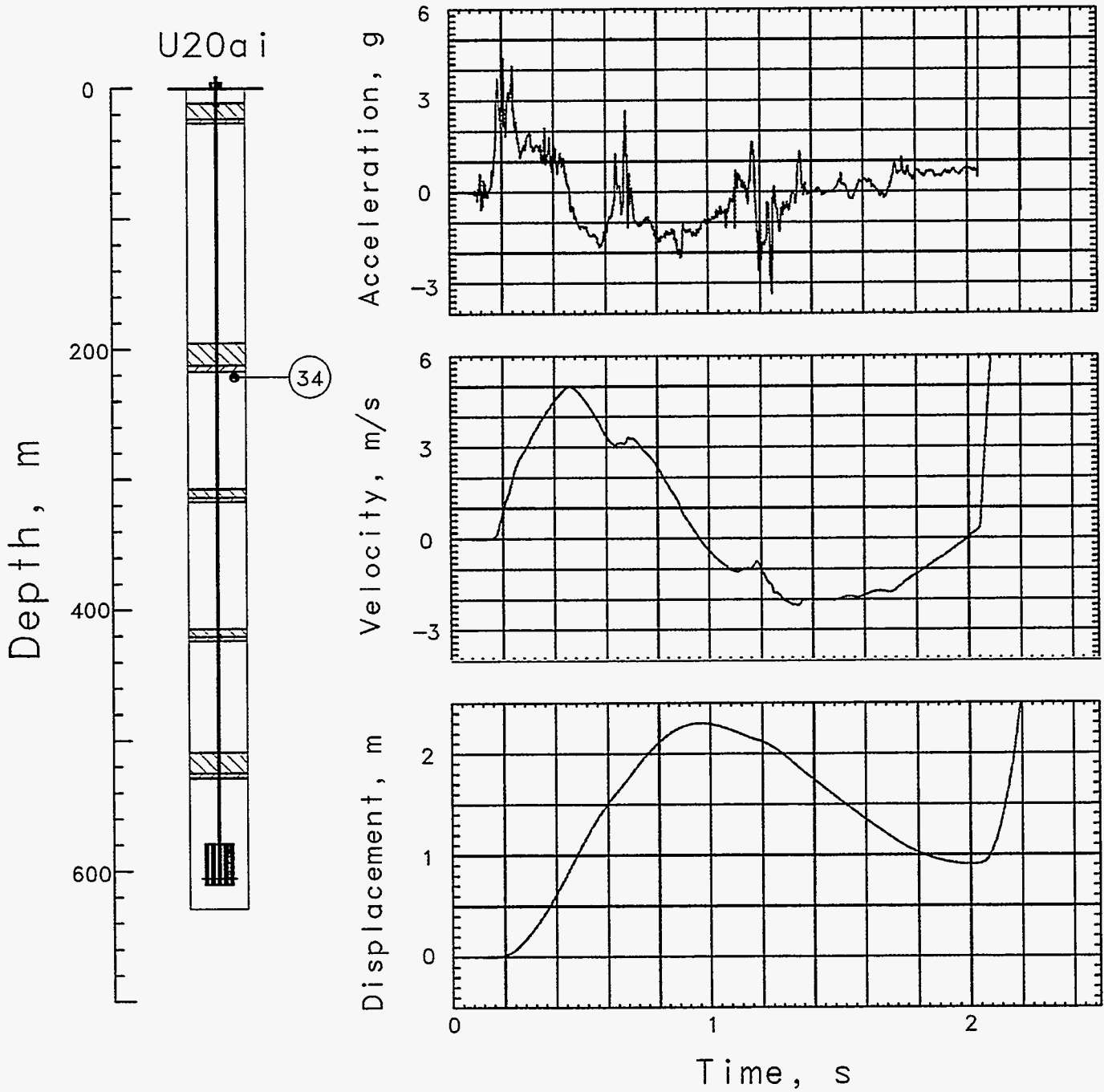


Figure 3.11 Explosion-induced vertical motion in the coarse stemming of the emplacement hole at a depth of 221.0 m (station 34). Station signals were lost at about 2.1 s after detonation.

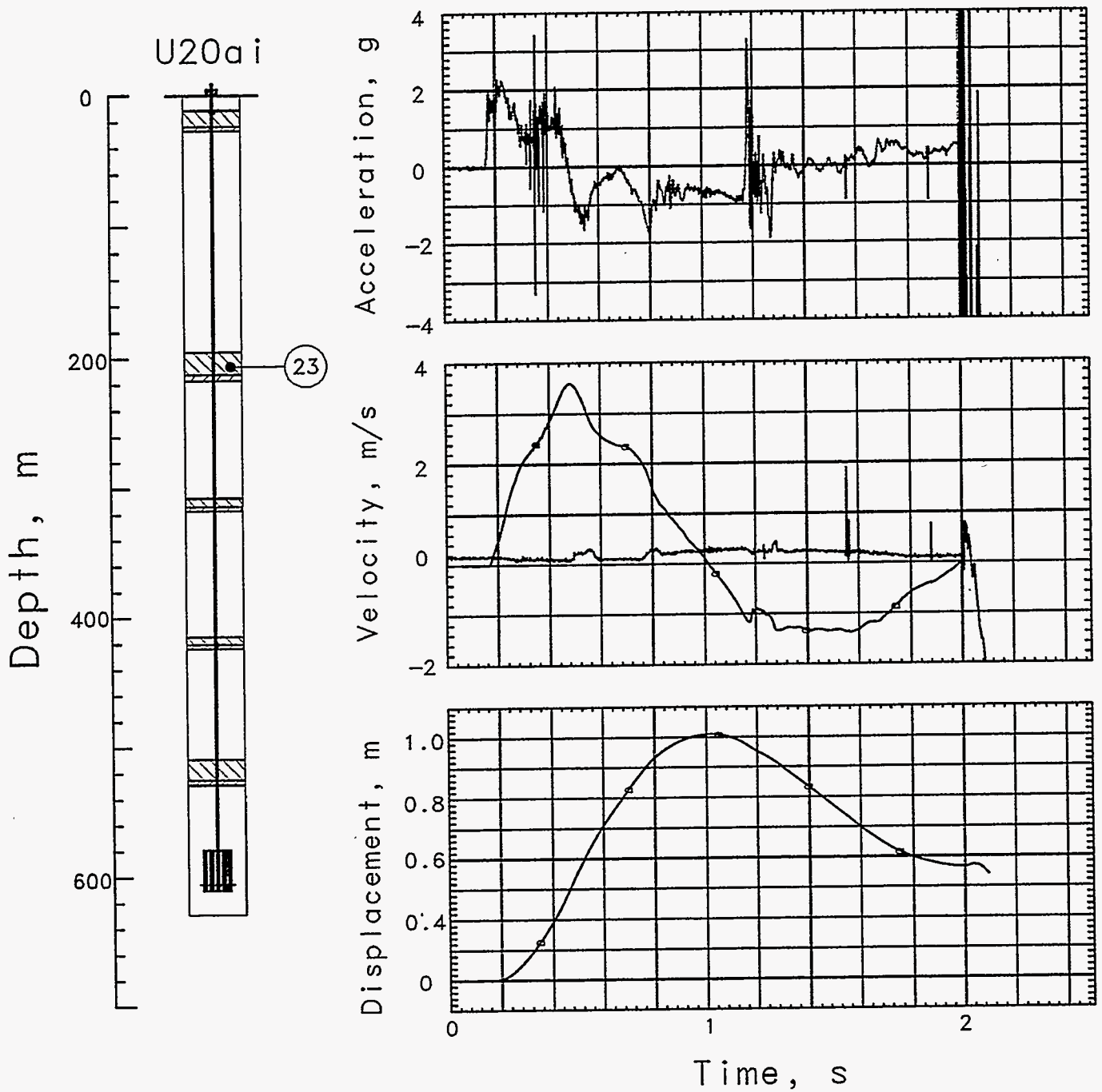


Figure 3.12 Explosion-induced vertical motion of the fourth plug at a depth of 207.3 m (station 23). Station signals were lost at about 2.0 s after detonation. Data records annotated with an "a" were obtained from an accelerometer. The associated velocimeter at this station was apparently inoperative pre-shot.

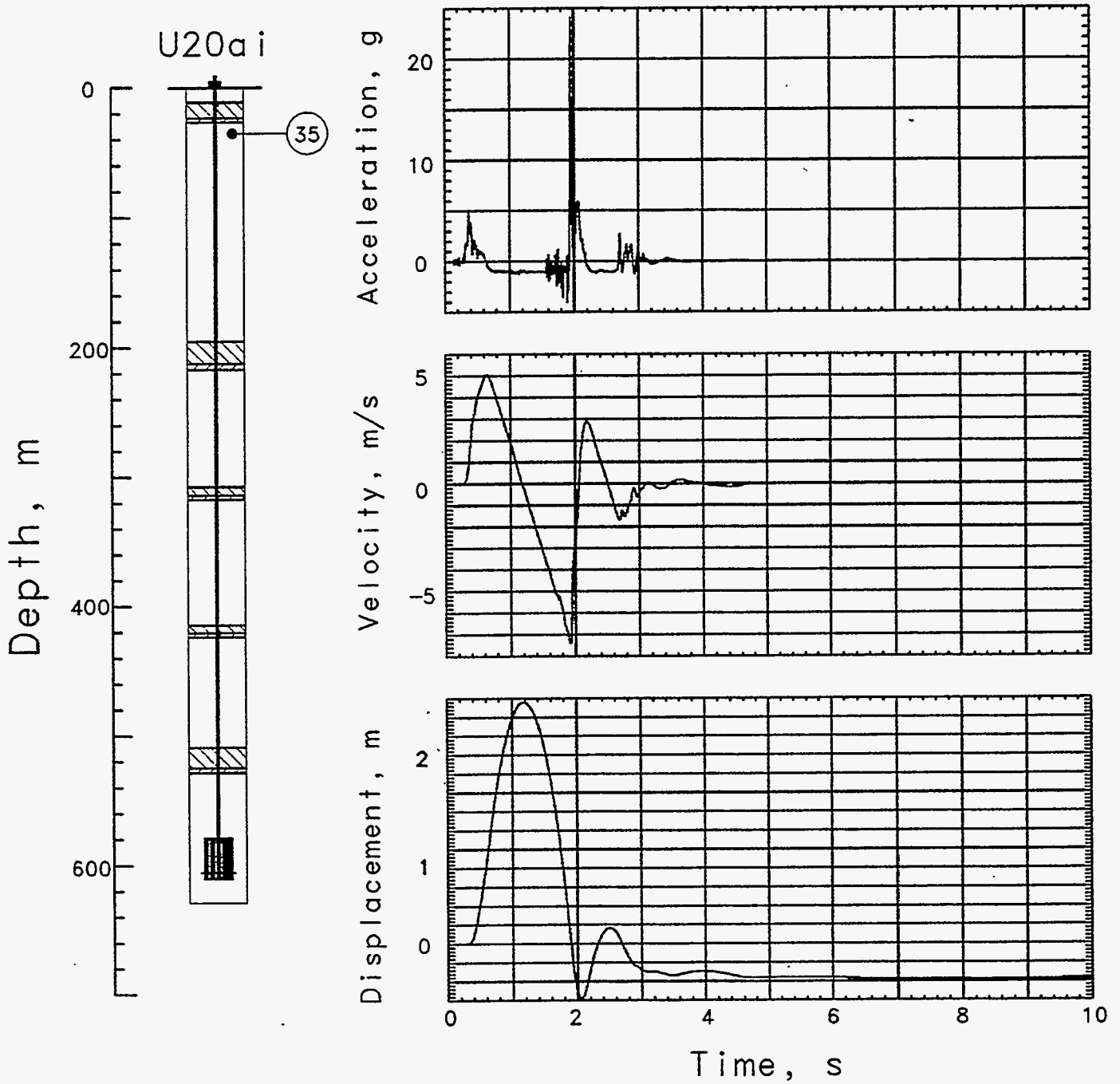


Figure 3.13 Explosion-induced vertical motion in the coarse stemming of the emplacement hole at a depth of 31.4 m (station 35). This is the only station for which the final explosion-induced displacement could be derived.

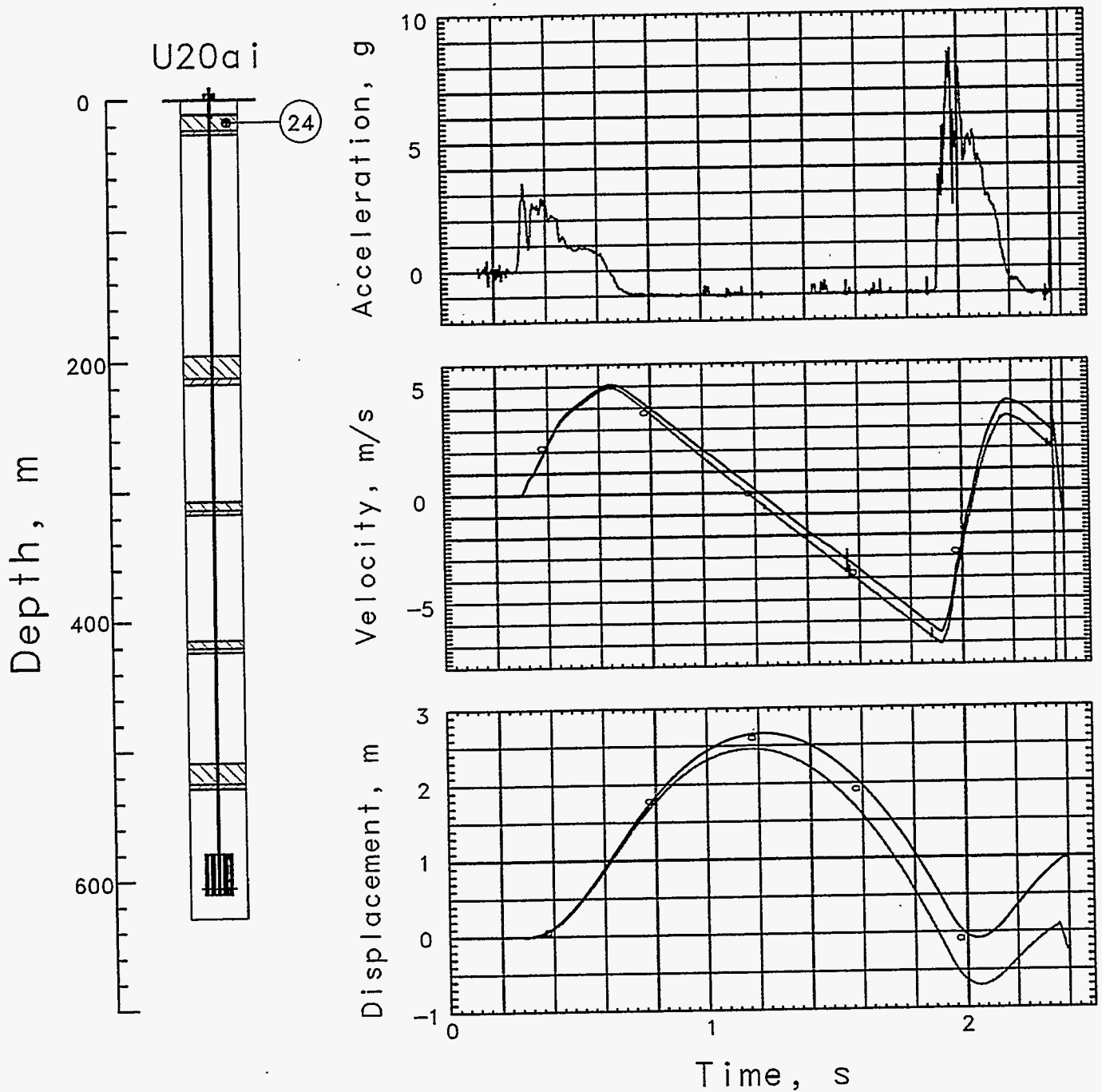


Figure 3.14 Explosion-induced vertical motion of the fifth plug at a depth of 17.7 m (station 24). Station signals were interrupted at about 2.4 s after detonation. Data records annotated with an "a" were obtained from an accelerometer.

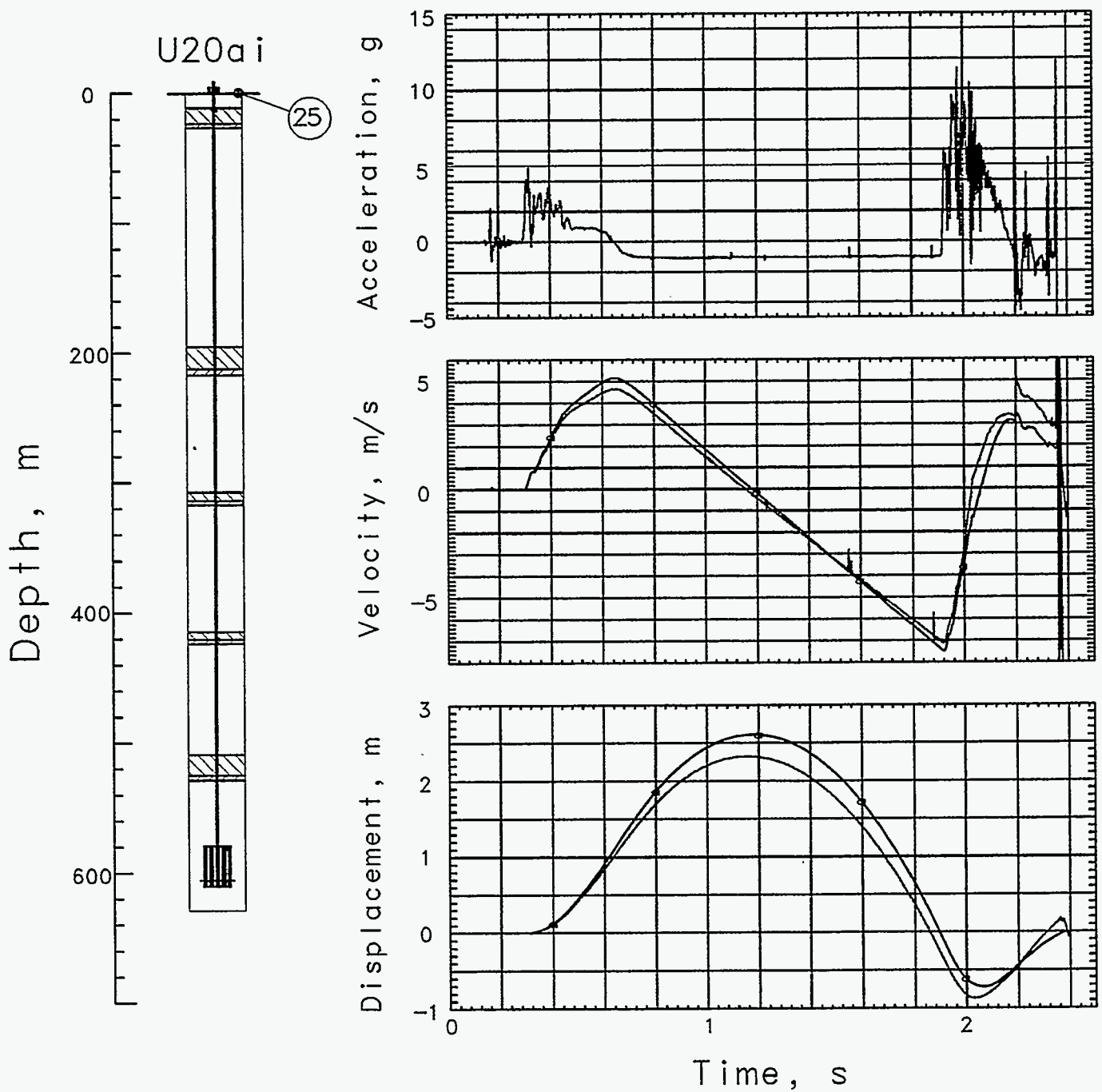


Figure 3.15 Explosion-induced vertical motion of the surface casing (station 25). Station signals were interrupted at about 2.4 s after detonation. Data records annotated with an "a" were obtained from an accelerometer.

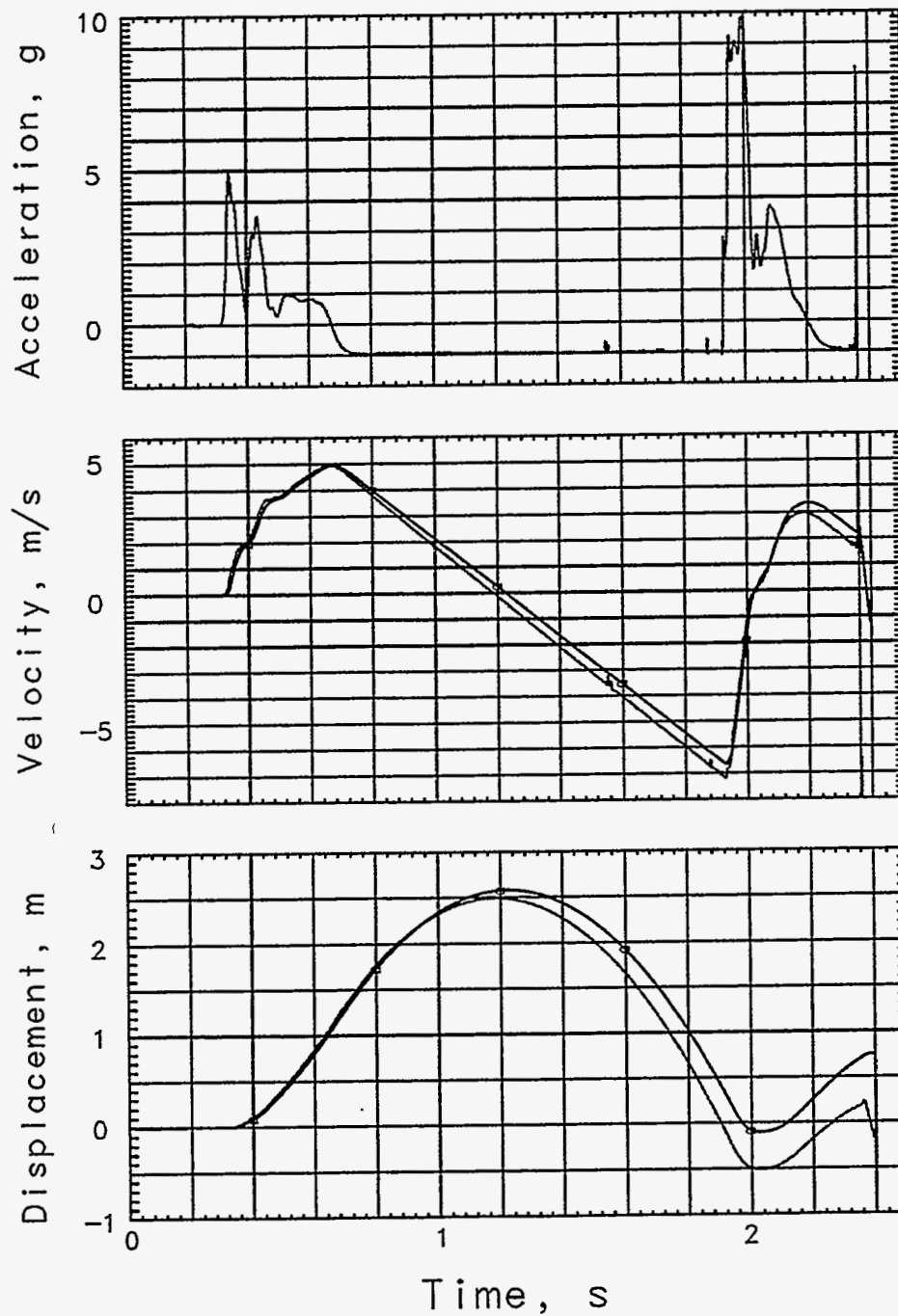


Figure 3.16 Explosion-induced vertical motion 0.91 m deep in the ground surface at a horizontal distance of 15.24 m from Surface Ground Zero (station 61). Station signals were interrupted at about 2.4 s after detonation. Data records annotated with an 'a' are derived from the accelerometer.

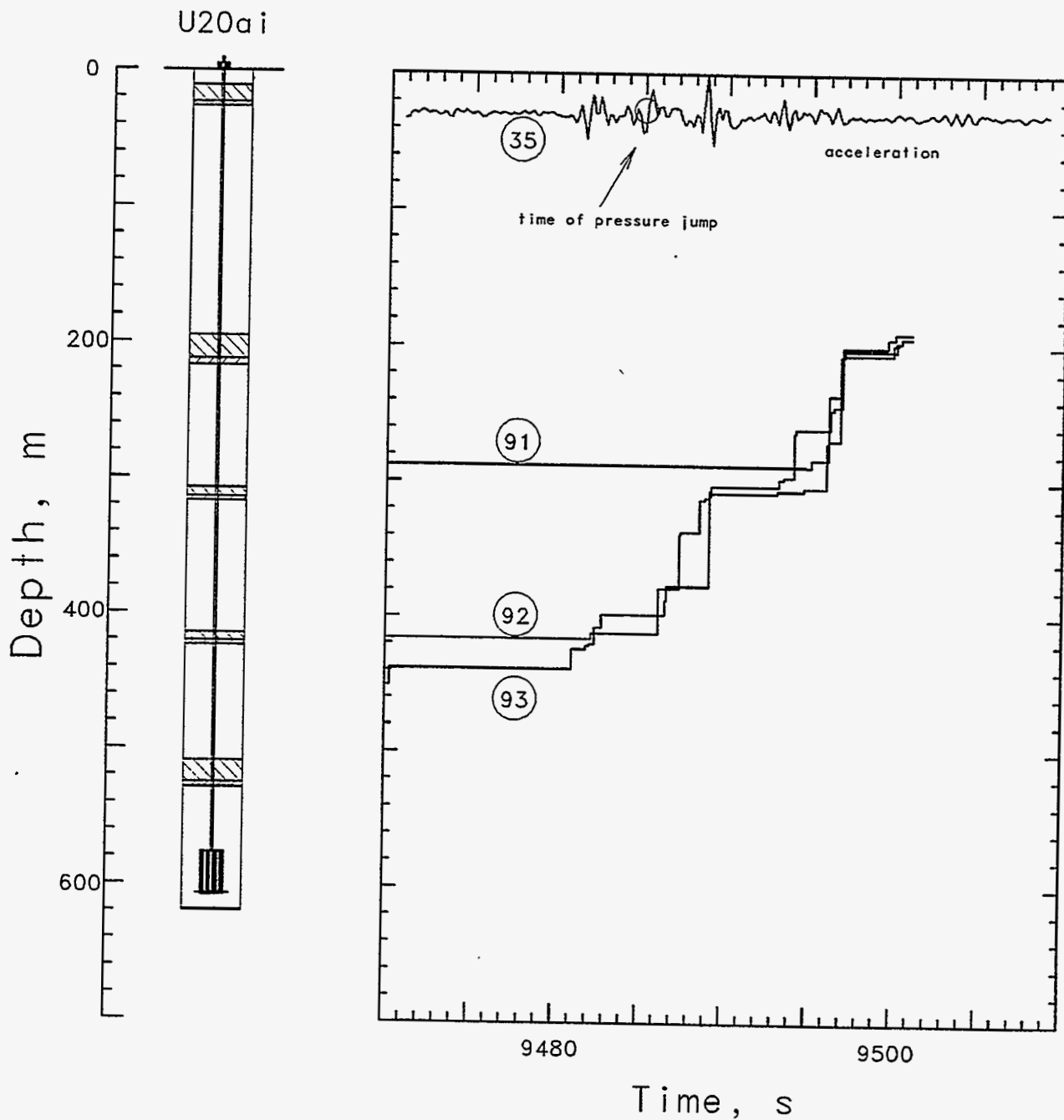


Figure 3.17 Collapse history as indicated by breaks in the EXCOR cables (stations 91, 92 and 93). The datum indicated by the circle indicates the time (9485 s) at which the pressure at station 35 increases by about 0.1 psi (see figure 3.5). Also shown is the acceleration history from station 35 at the approximate depth of the station (see figure 3.18).

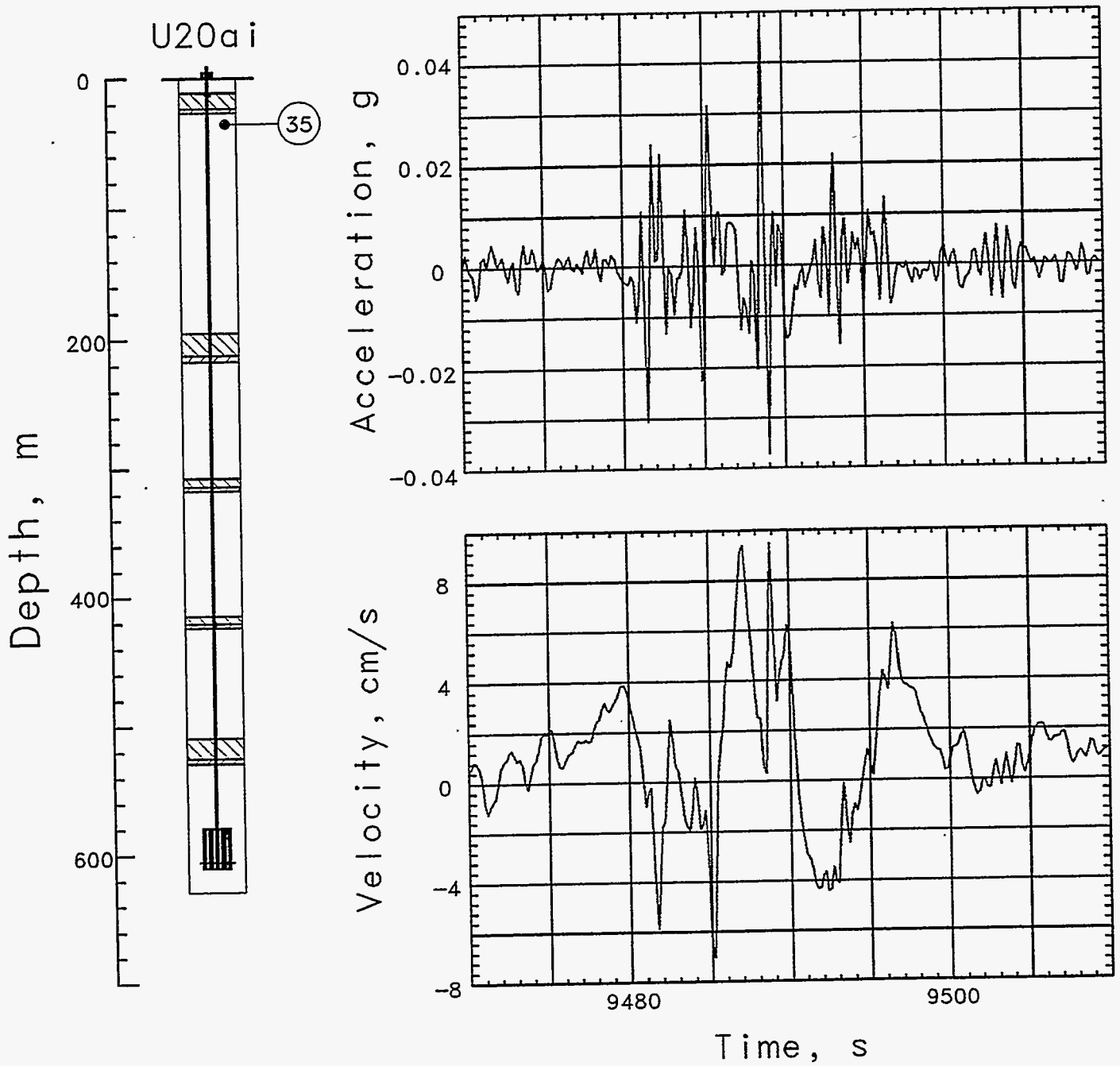


Figure 3.18 Collapse-induced vertical motion in the coarse stemming of the emplacement hole at a depth of 31.4 m (station 35). The acceleration is integrated once to velocity: the record is not of good enough quality to obtain meaningful displacement.

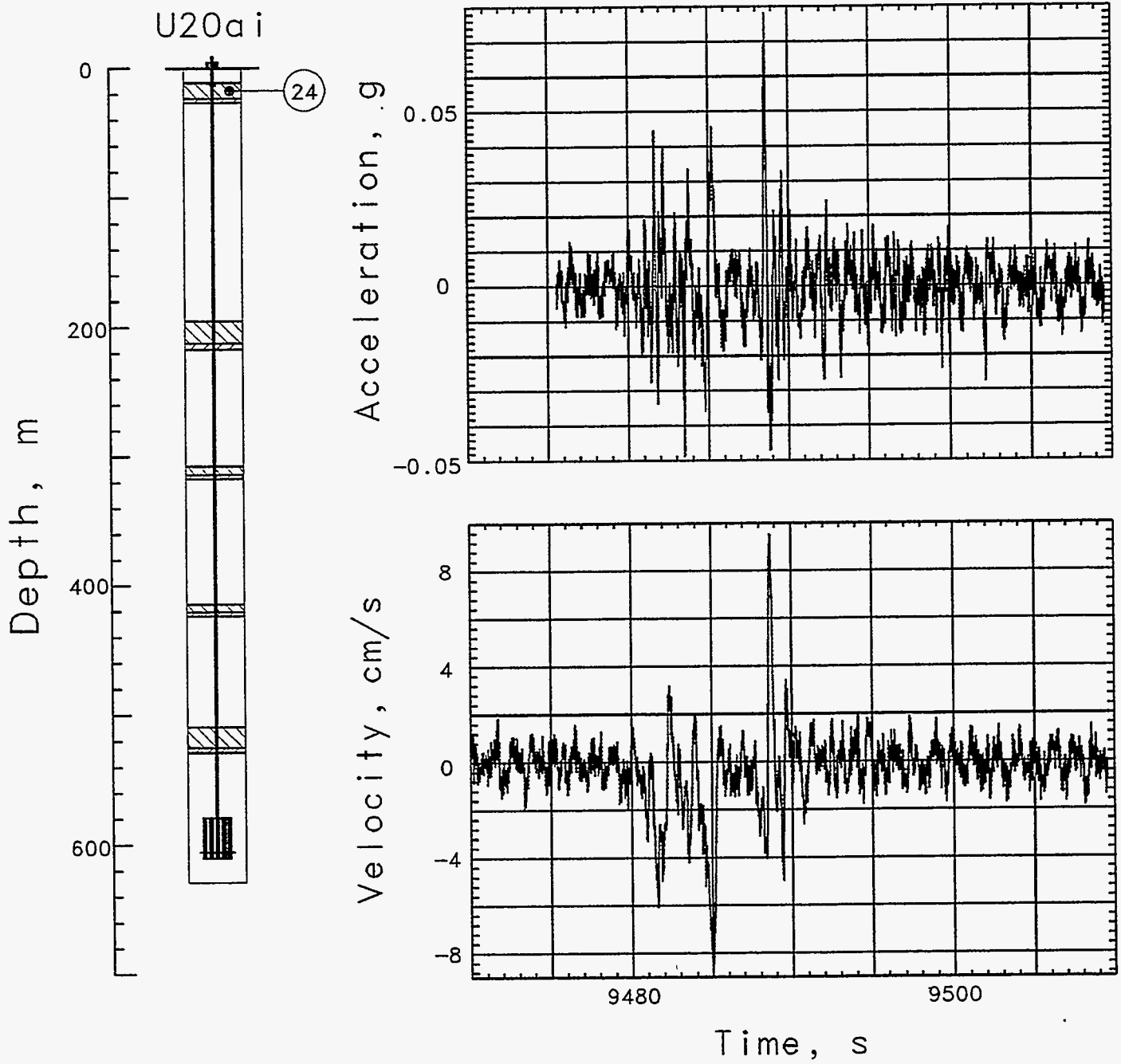


Figure 3.19 Collapse-induced vertical motion of the top plug at a depth of 17.7 m (station 24). Only the measured acceleration and velocity are presented.

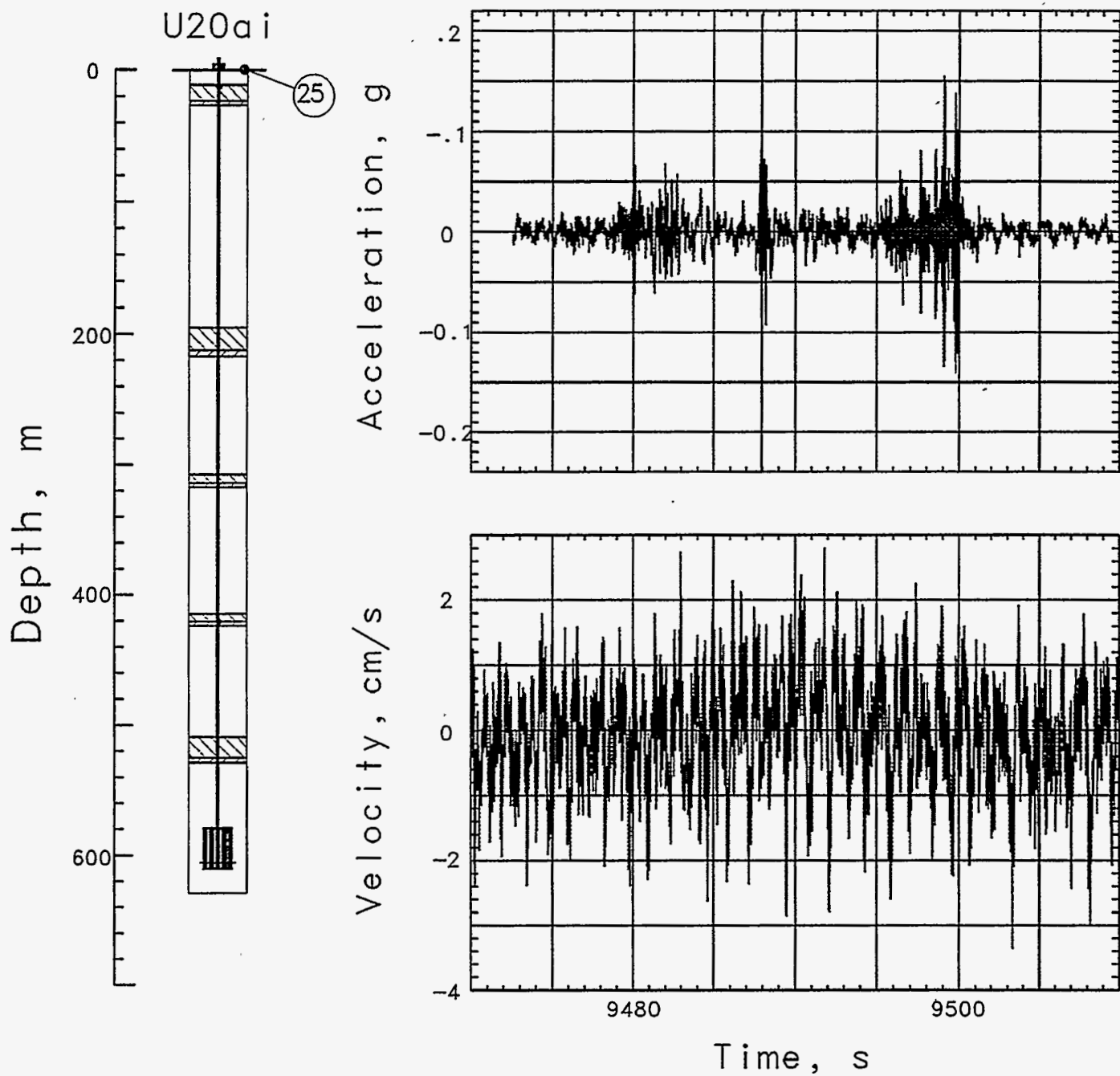


Figure 3.20 Collapse-induced vertical motion of the surface casing (station 25). Only the measured acceleration and velocity are presented.

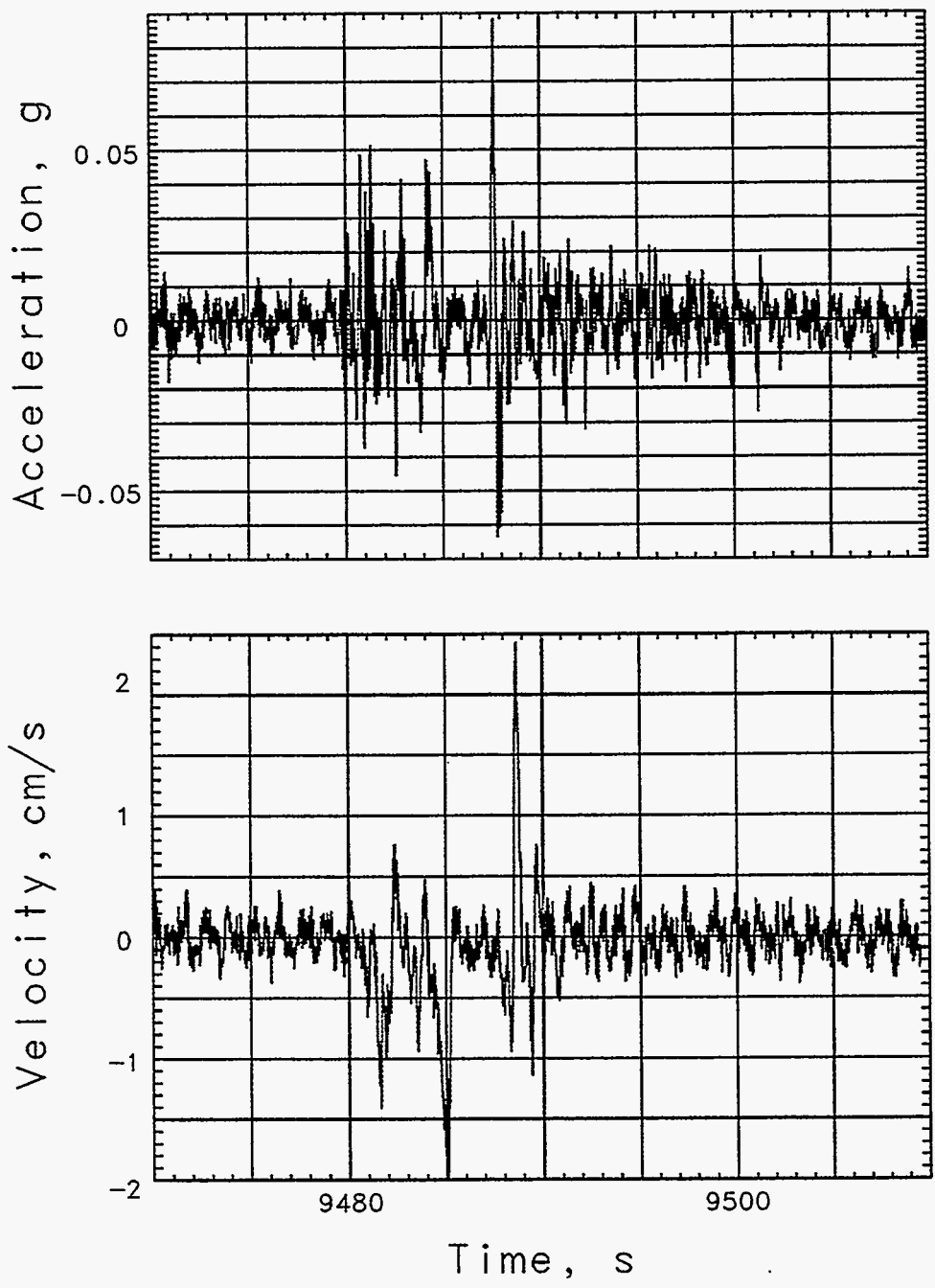


Figure 3.21 Collapse-induced vertical motion 0.91 m deep in the ground surface at a horizontal distance of 15.24 m from Surface Ground Zero (station 61). Only the measured acceleration and velocity are presented.

4. Other Measurements

4.1 Motion in the LLNL trailer park

Figure 4.1 shows data as recorded on a high sensitivity accelerometer and a geophone mounted in the ground surface of the trailer park (station 62). Included is the entire recording period from a few minutes before detonation to a few minutes after subsurface subsidence. The low seismic activity from JEFFERSON is evident from these records.

Triaxial motion of the recording trailer is shown in figures 4.2–4.4. Motion sensed during the collapse episode at about 5740 s was of too low an amplitude for meaningful reduction and is not shown.

4.2 Permeability data

As part of a continuing investigation of the permeability of the upper geologic layers of the Nevada Test Site, sensitive pressure transducers were fielded in the emplacement hole beneath each of the two upper SGC plugs. One station was below the fifth plug and two were in the coarse stemming beneath the top plug and a fourth was placed 0.61 m deep in the ground surface 15.2 m from Surface Ground Zero. Data were digitally recorded from about 2 months prior to the event to event time and are shown in figure 4.5.

4.2 Stress and strain

Radial and transverse stress and strain were monitored at two locations in the bottom plug using transducers (developed by Dynasen, Inc.⁶) which, in principal, allow the removal of the strain contribution to the record of the stress transducer. Each location was monitored with transducer packages, each containing two elements (one being Ytterbium and the other constantan) having initial unstrained resistances of about 300 Ω . The elements were coupled to the stress field with a thin layer of fluid in an attempt to preclude inhomogenities introduced by the required cladding on the package. Figures 4.5 and 4.6 show the fractional resistance change ($\% \Delta R/R$) histories obtained from these instruments. Only three of the eight elements between these two stations survived the shock arrival (at about 48 ms) with all signals being lost just after 100 ms. The EMP introduced a large signal component on each of the channels, lasting at least until shock arrival. This casts doubt on the usefulness of the information from those elements that survived the shock.

Table 4.1 Summary of Motion

| Gauge | Slant Range (m) ^(a) | Arrival Time (ms) | Peak Acceleration (g) | Peak Velocity (m/s) | Peak Displacement (m) | Residual Displacement (cm) |
|-------|-----------------------------------|----------------------|-----------------------------|---------------------------|-----------------------------|----------------------------------|
| 71av | 680 ^(a) | 398 | 2.1, 3.4 ^(b) | 1.6 | 0.60 | (c) |
| 71uv | | - | - | 2.4 | 0.48 | -15 |
| 71ar | 680 ^(a) | 387 | 3 | 0.9 | 0.67 | (c) |
| 71ur | | - | - | 1.4 | 1.13 | (c) |
| 71at | 680 ^(a) | 385 | 0.7 | 0.1, 0.27 | 0.06 ^(c) | (c) |
| 71ut | | - | - | 0.08, 0.25 | 0.033 ^(c) | (c) |

(a) Range is approximate: stations are in recording trailer.

(b) Slap-down peak.

(c) Signal lost before final value attained.

Table 4.2 Accelerometer Characteristics

| Gauge | Natural Frequency (Hz) | Damping Ratio | System Range (g's) |
|-------|---------------------------|---------------|-----------------------|
| 71av | 330 | 0.70 | 20 |
| 71ar | 340 | 0.70 | 15 |
| 71at | 310 | 0.75 | 15 |

Table 4.3 Velocimeter Characteristics

| Gauge | Natural Frequency (Hz) | Time to 0.5 Amplitude (s) | Calibration Temperature (°C) | Operate Temperature (°C) | System Range (m/s) |
|-------|------------------------------|---------------------------------|------------------------------------|--------------------------------|--------------------------|
| 71uv | 3.253 | 12.03 | 24.42 | 18.75 | 7 |
| 71ur | 3.516 | 9.59 | 24.74 | 18.75 | 5 |
| 71ut | 3.354 | 8.87 | 25.41 | 18.75 | 5 |

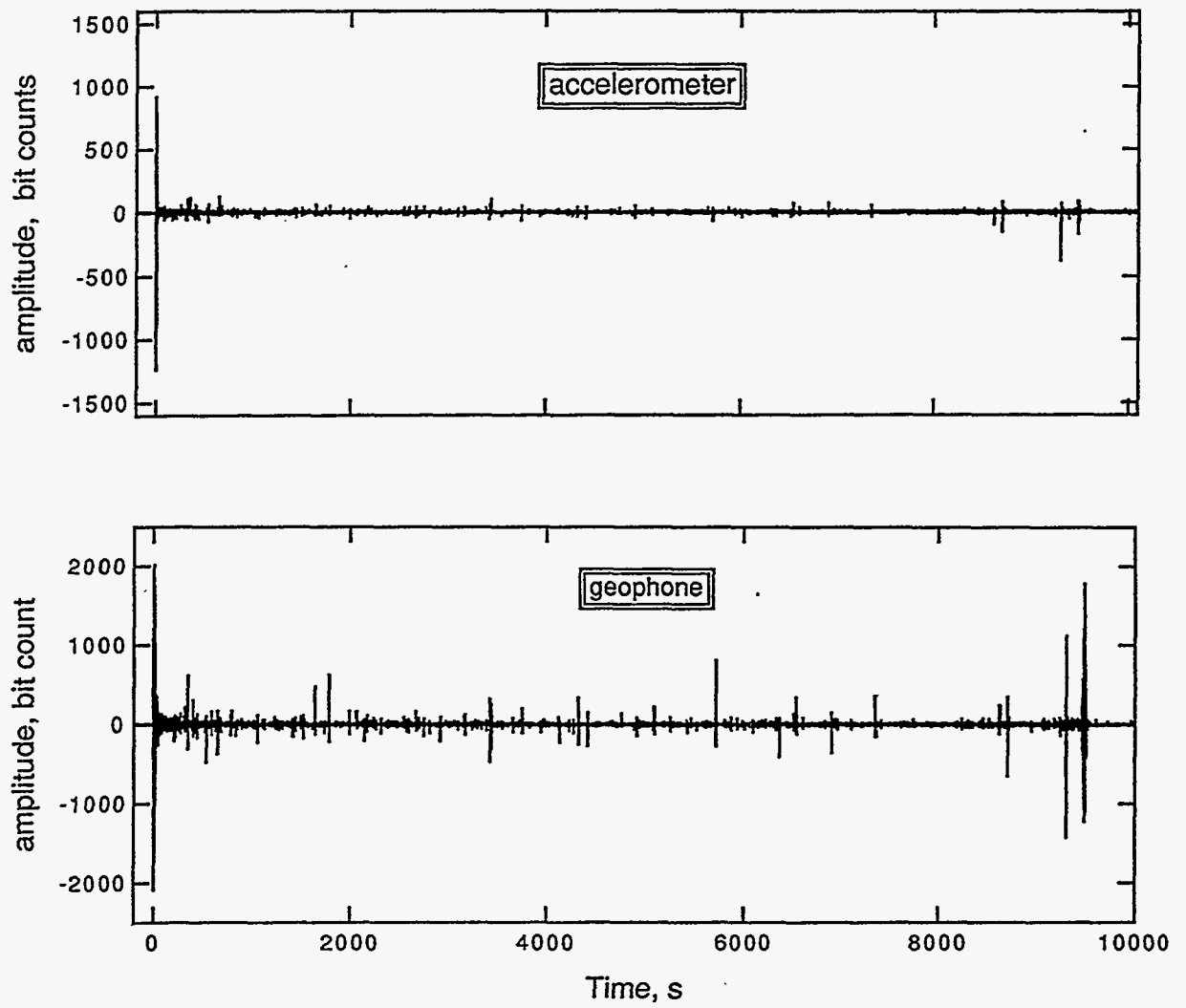


Figure 4.1 Data from the vertical geophone and sensitive accelerometer mounted in the ground surface at the recording trailer (station 62). Subsurface subsidence to a depth of about 190 m occurred at about 2hr, 37min.

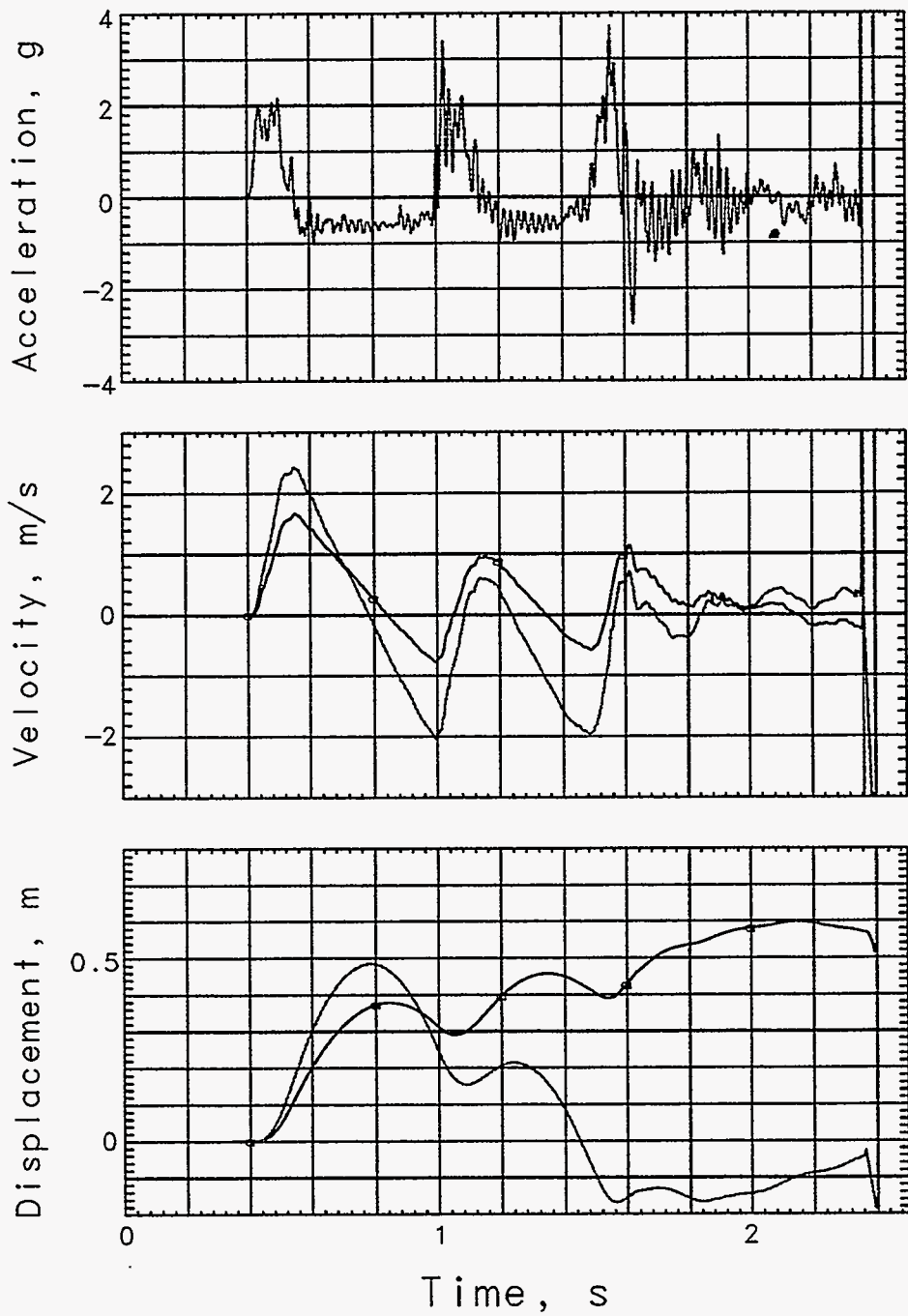


Figure 4.2 Explosion-induced vertical motion of the recording trailer (station 71). Data records annotated with an 'a' are derived from the accelerometer. Station signals were interrupted at about 2.4 s after detonation.

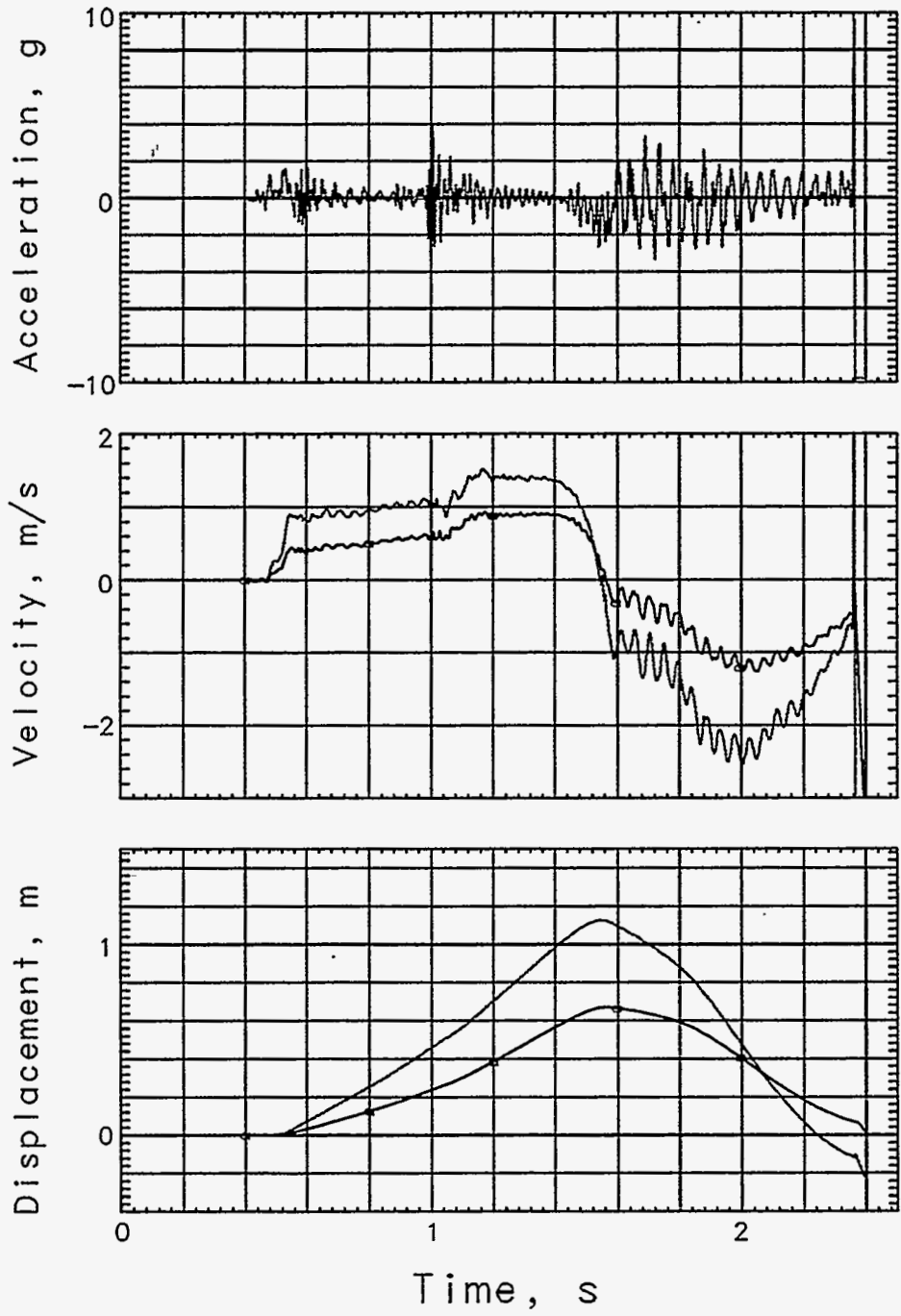


Figure 4.3 Explosion-induced horizontal-radial motion of the recording trailer (station 71). Data records annotated with an 'a' are derived from the accelerometer. Station signals were interrupted at about 2.4 s after detonation.

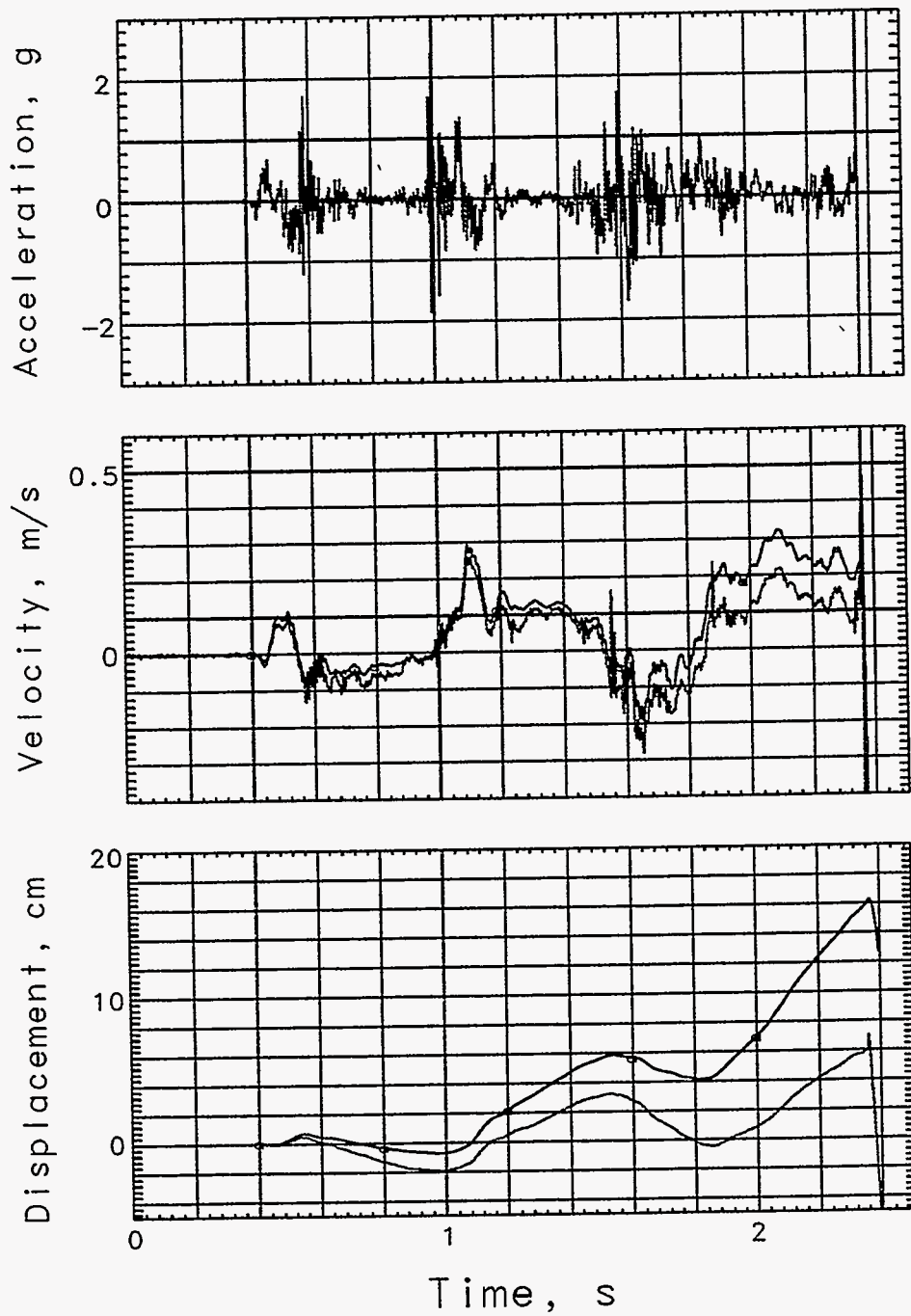


Figure 4.4 Explosion-induced horizontal-transverse motion of the recording trailer (station 71). Data records annotated with an 'a' are derived from the accelerometer. Station signals were interrupted at about 2.4 s after detonation.

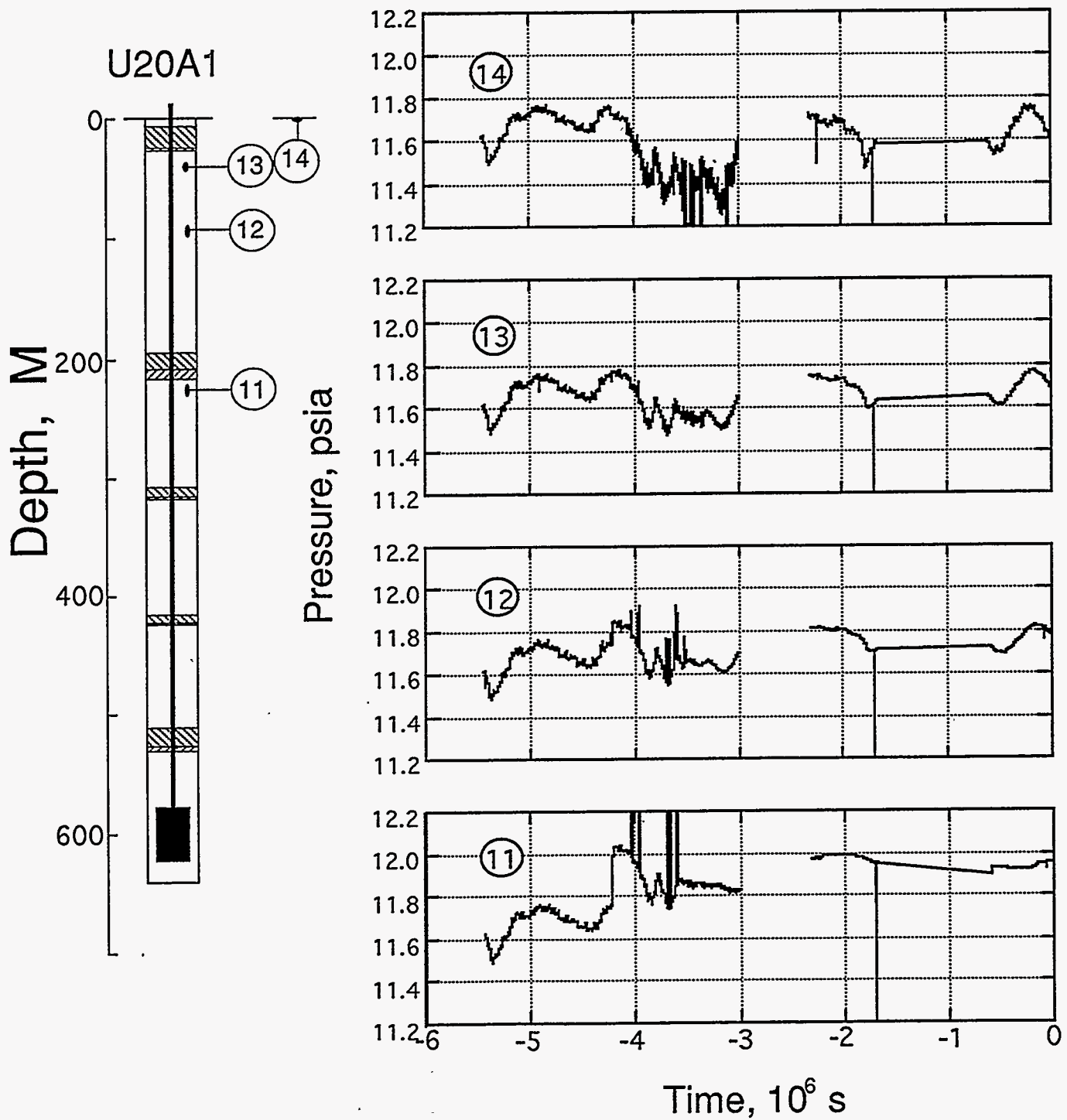


Figure 4.5 Permeability pressure data measured in hole U20ai prior to the event. Time is relative to the event.

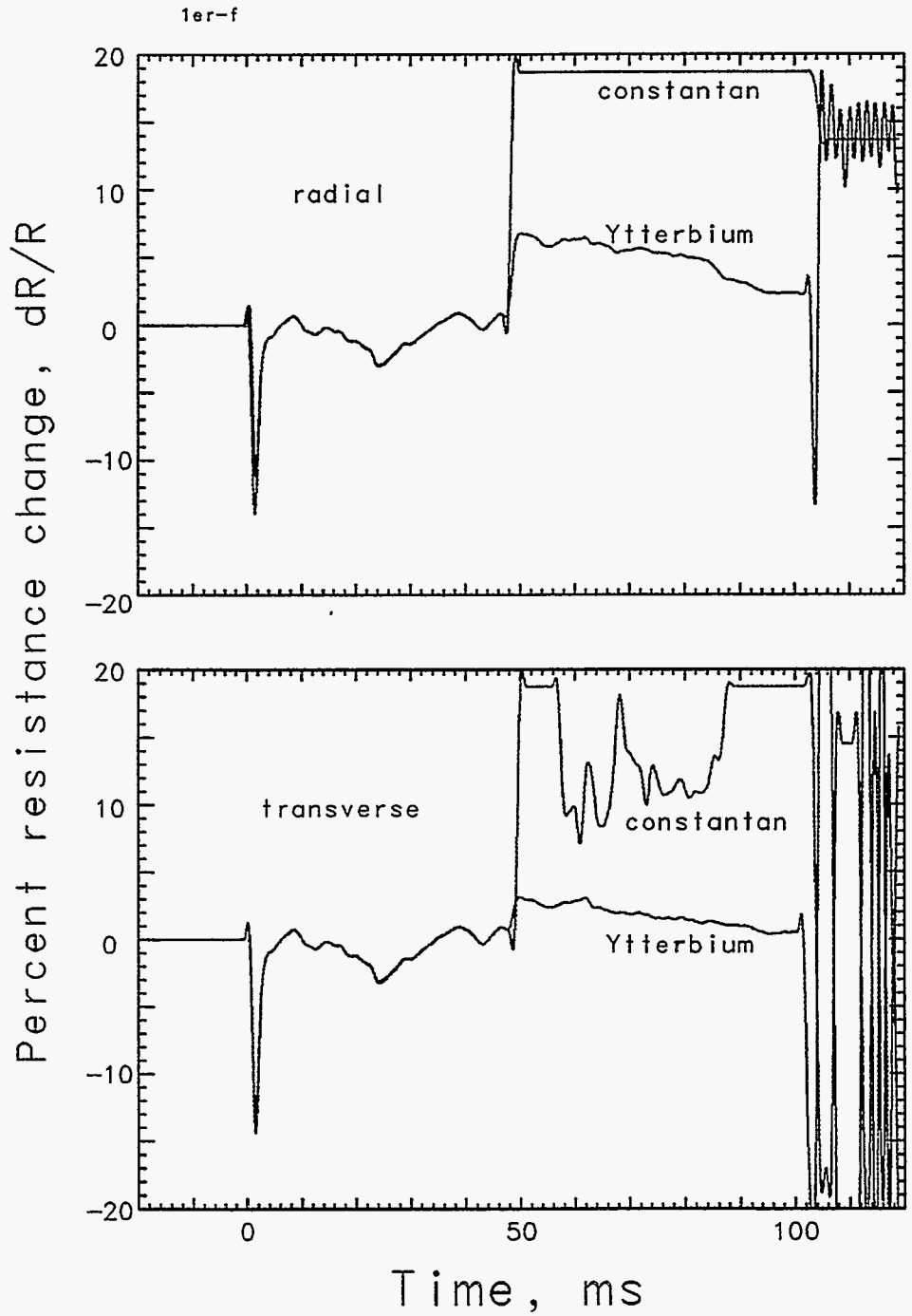


Figure 4.6 Output from the two element stress & strain transducers mounted to sense radial and transverse information at a range of 94.1 m from the working point (station 1). The signal prior to 48 ms is due to system excitation from the EMP. Both stress and strain signals are lost shortly after 0.1 s

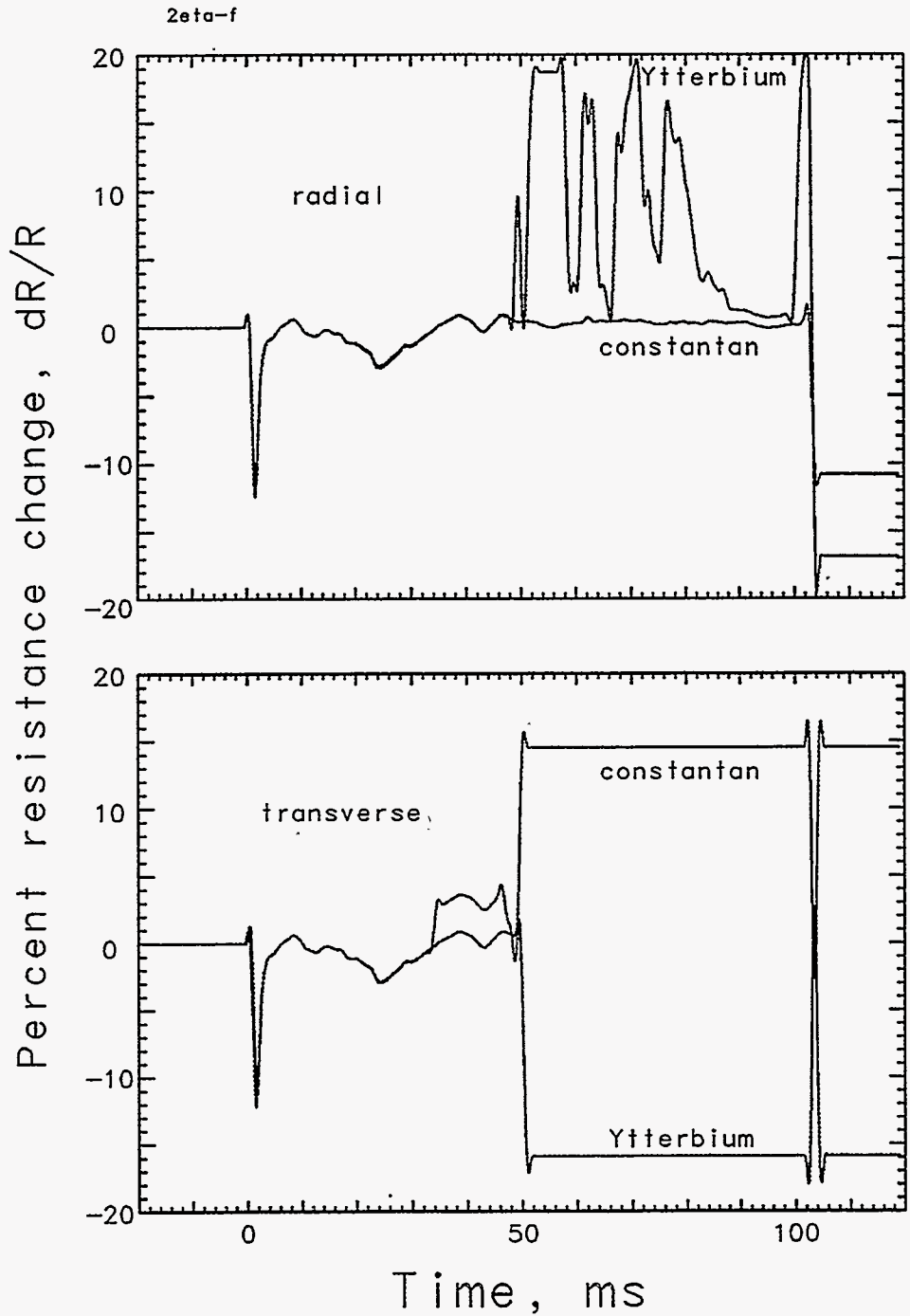


Figure 4.7 Output from the two element stress & strain transducers mounted to sense radial and transverse information at a range of 95.6 m from the working point (station 2). The signal prior to 48 ms is due to system excitation from the EMP. Both stress and strain signals are lost shortly after 0.1 s

References

1. J. L. Wagoner, "U20ai Site Characteristics Report", CP 85-86, Lawrence Livermore National Laboratory, Livermore, CA, October 14, 1985.
2. Alfred R. Burer, "Containment Report for U20ai", Holmes & Narver, Inc., NTS:A2:86-23, March 31, 1986.
3. LLNL contact for additional information: R. Heinle (CORRTEX data).
4. J. Kalinowski, T. Stubbs, L. Davies, and B. Hudson, "Recent stress gage developments", Range Commanders Council, Telemetry Group, 4-6 July, 1985, Monterey, California.
5. Richard A. Spilsbury, "Special Measurements Final Engineering Report for JEFFERSON, U20ai," EG&G, Energy Measurements, Las Vegas, NV, SM:86E-133-35, 13 May 1986.
6. Richard A. Spilsbury, "Special Measurements Physics/Instrumentation package for JEFFERSON, U20ai, Revision 'A'" EG&G, Energy Measurements, Las Vegas, NV, SM:86E-133-36, 13 May, 1986.
7. J. A. Kalinowski, "JEFFERSON Stress Gage Report", EG&G, Energy Measurements, Pleasanton, CA, JAK 92-12, April 14, 1992.

Distribution:

LLNL

| | |
|----------------------|-------|
| TID (11) | L-053 |
| Test Program Library | L-045 |
| Containment Vault | L-221 |
| Burkhard, N. | L-221 |
| Cooper, W. | L-049 |
| Denny, M. | L-205 |
| Dong, R. | L-140 |
| Goldwire, H. | L-221 |
| Heinle, R. (5) | L-221 |
| Mara, G. | L-049 |
| Moran, M.T. | L-777 |
| Moss, W. | L-200 |
| Olsen, C. | L-221 |
| Patton, H. | L-205 |
| Pawloski, G. | L-221 |
| Rambo, J. | L-200 |
| Roland, K. | L-221 |
| Roth, B. | L-049 |
| Valk, T. | L-154 |
| Yunker, L. | L-203 |

LANL

| | |
|-------------|-------|
| App, F. | F-659 |
| Brunish, W. | F-659 |
| Kunkle, T. | F-665 |
| Trent, B. | F-664 |

Sandia

| | |
|----------------|---------|
| Chabai, A. | MS-1159 |
| Smith, Carl W. | MS-1159 |

EG&G/AVO

| | |
|-------------|-----|
| Brown, T. | A-5 |
| Gilmore, L. | A-1 |
| Hatch, M. | A-5 |
| Still, G. | A-5 |
| Stubbs, T. | A-5 |

EG&G/NVO

| | |
|--------------|---------|
| Bellow, B. | N 13-20 |
| Davies, L. | N 13-20 |
| Moeller, A. | N 13-20 |
| Robinson, R. | N 13-20 |
| Webb, W. | N 13-20 |

DNA

Ristvet, B.

S-Cubed

Peterson, E.

Eastman Cherrington Environment
1640 Old Pecos Trail, Suite H
Santa Fe, NM 87504

Keller, C.